On the Performance of MRC Receiver with Unknown Timing Mismatch-A Large Scale Analysis

Mehdi Ganji, *Student Member, IEEE,* Hamid Jafarkhani, *Fellow, IEEE*

Abstract

There has been extensive research on large scale multi-user multiple-input multiple-output (MU-MIMO) systems recently. Researchers have shown that there are great opportunities in this area, however, there are many obstacles in the way to achieve full potential of using large number of receive antennas. One of the main issues, which will be investigated thoroughly in this paper, is timing asynchrony among signals of different users. Most of the works in the literature, assume that received signals are perfectly aligned which is not practical. We show that, neglecting the asynchrony can significantly degrade the performance of existing designs, particularly maximum ratio combining (MRC). We quantify the uplink achievable rates obtained by MRC receiver with perfect channel state information (CSI) and imperfect CSI while the system is impaired by unknown time delays among received signals. We then use these results to design new algorithms in order to alleviate the effects of timing mismatch. We also analyze the performance of introduced receiver design, which is called MRC-ZF, with perfect and imperfect CSI. For performing MRC-ZF, the only required information is the distribution of timing mismatch which circumvents the necessity of time delay acquisition or synchronization. To verify our analytical results, we present extensive simulation results which thoroughly investigate the performance of the traditional MRC receiver and the introduced MRC-ZF receiver.

Index Terms

Timing mismatch, multi-user MIMO, massive MIMO, MRC, over sampling

M. Ganji and H. Jafarkhani are with the Center for Pervasive Communications and Computing, University of California, Irvine, CA, 92697 USA (e-mail: {mganji, hamidj}@uci.edu). This work was supported in part by the NSF Award CCF-1526780.

I. Introduction

Introducing multiple-input multiple-output (MIMO) systems was a breakthrough in communication systems which was studied extensively during the past two decades [1]–[3]. Using multiple antennas at transmitter and receiver provides the opportunity to increase the capacity and improve the performance significantly [4], [5]. One of the applications of MIMO systems is in multiuser scenarios where K users, each equipped with multiple antennas communicate with a common multiple antenna receiver. Beside traditional problems in point to point communication, due to distributed nature of multiuser-MIMO (MU-MIMO) systems, new challenges exist like timing mismatch between received signals from different users [6]. When the number of users and number of receive antennas are moderate, this issue is often handled by synchronization methods [7]–[9]. Recently, it has been shown that timing mismatch can even improve the performance when the time mismatch values are known by the receiver and proper sampling and detection methods are used [10]–[14]. However, increasing the number of receive antennas and users makes the time delay estimation or synchronization challenging and even impractical, especially in the context of massive MIMO systems [15].

In large scale MU-MIMO systems, the base station is equipped with very large number of receive antennas and communicates with tens of users at the same time and frequency. The benefits of massive MIMO settings including, near optimal performance using simple processing like maximum ratio combining (MRC), increased spectral efficiency and energy efficiency, have been studied in the literature [16]–[18]. However, there are many challenges which need to be addressed before the gains can be realized in practice [19], [20]. For hundreds of receive antennas, one major challenge is the fact that it is impossible to receive perfectly aligned signals at all the receive antennas. Therefore, it is of great importance to investigate timing mismatch in large scale MU-MIMO systems. For large scale multi-carrier MU-MIMO systems, the timing mismatch between the received signals can be modeled as the phase rotation of the received symbols. Such a phase rotation behaves similar to the phase noise introduced by the oscillator at the receiver and has been studied in the literature [21], [22]. However, to the best of our knowledge, there is no work in the literature to consider the timing mismatch in single-carrier massive MIMO scenarios. In [23], it is shown that using single carrier transmission can achieve near optimal sum rate. The authors have proposed a simple precoding which mitigates the intersymbol interference (ISI) caused by channel multipath. However, they assume perfect symbol level alignment enabling

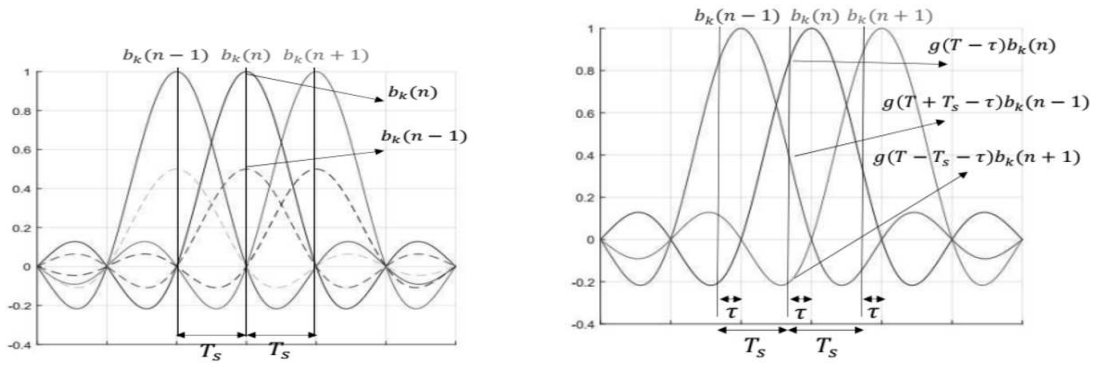

(a) ISI caused by multipath channel

(b) ISI caused by imperfect sampling

Fig. 1: Demonstration of two different sources of creating ISI

perfect sampling at the peak point of the transmitted pulse shape which might be challenging in a large scale MU-MIMO system. Inevitable timing mismatch between received signals, results in imperfect sampling, and hence creates another source of ISI as illustrated in Fig. 1.

In Fig. 1a, the ISI is created by dotted symbols which are delayed copies of the transmitted symbols caused by a frequency selective channel. In Fig. 1b, the ISI is generated by imperfect sampling. Note that imperfect sampling is unavoidable when the received signals are not aligned. If the timing mismatch values are known at the receiver, it can obtain ISI-free samples for each user by oversampling as many times as the number of users, as explained in [14]. However, considering practical challenges for delay acquisition in a large scale MU-MIMO system, we assume that the timing mismatch values are unknown and the receive only knows their distribution. In this work, we will investigate the effect of timing mismatch in the performance of MRC receiver. We consider flat fading Rayleigh fading channels to reveal the main concepts; however, the results can be generalized to frequency selective channels which is the topic of our future work.

It is shown in the literature that in large scale MU-MIMO systems, a low complexity MRC receiver can approach near optimal performance and even outperform its complex counterparts, i.e., ZF and MMSE receivers, at low SNR [17]. An MRC receiver also follows the power scaling law which roughly indicates that to maintain the same quality-of-service as with a single-antenna BS, the transmit power of a 100-antenna BS would be only almost 1% of the power of the single-antenna system [24]. As we shall see, ignoring the asynchrony can significantly

degrade the performance of the MRC receiver (and expectedly other existing receiver designs). We develop a mathematical model that explicitly accounts for the timing mismatch among the received signals. It then quantifies the detrimental impact of asynchrony on the MRC receiver, and suggests how to mitigate it by making some modifications to the MRC receiver. The paper makes the following specific contributions:

- We derive a tight approximation for the achievable uplink rate using the MRC receiver in the presence of timing mismatch. We consider a single cell scenario with perfect and imperfect CSI. Our results are general and cover any arbitrary delay distribution including the synchronous scenario.
- We find the optimal sampling times which maximize the asymptotic achievable rate by the MRC receiver when the number of receive antennas goes to infinity.
- We show that the MRC receiver cannot provide the power scaling law when there is misalignment between received signals.
- We introduce a new receiver design called MRC-ZF which alleviates the effects of timing mismatch and follows the power scaling law.
- We derive an achievable uplink rate approximation when the MRC-ZF receiver is used.

The rest of the paper is organized as follows: first we introduce the system model in Section II. Then we explain discretization and receiver processes in Section III. We analyze the achievable rates obtained by the MRC receiver when unknown delays exist in Section IV and the MRC-ZF receiver structure is presented for two scenarios: perfect CSI and estimated CSI. Next, simulation results are presented in Section V to verify the effectiveness of our proposed methods. Finally, we summarize our contributions in Section VI.

II. System Model

We consider a system with K users, transmitting data to a common receiver with M receive antennas simultaneously where M is very large and tends to infinity. Due to different physical locations of users, their signal is received with various time delays. It is assumed that each data stream is received with an arbitrary delay smaller than the symbol interval. The signal transmitted from User k is described by:

$$s_k(t) = \sqrt{\rho_d} \sum_{i=1}^{N} b_k(i) p(t - (i-1)T_s) \tag{1}$$

where T_s, ρ_d and $p(.)$ represent the symbol length, the transmit power, and the pulse-shaping filter with non-zero duration of T, respectively. Also, N is the frame length and $b_k(i)$ is the transmitted symbol by User k in the ith time slot. The transmitted signals are received with a relative delay of ς_{km} and a channel path gain of $c_{km} = \sqrt{\beta_k} h_{km}$. In channel path gains, $\sqrt{\beta_k}$ shows path loss that depends on the distance between the corresponding user and the base station and h_{km} represents fading coefficients which are usually modeled as Rayleigh distribution with zero mean and variance one. Channel path gains are assumed to be fixed during the transmission of each frame. Then, the continuous received signal at the mth receive antenna can be represented by:

$$\psi_m(t) = \sqrt{\rho_d} \sum_{k=1}^{K} c_{km} s_k(t - \varsigma_{km}) + \nu_m(t) \tag{2}$$

where K is the number of users and $\nu_m(t)$ is the white noise with zero mean and variance one. The relative delays among users can be separated in two parts: one for frame level asynchrony and the other for symbol level asynchrony, i.e, $\varsigma_{km} = d_{km} T_s + \tau_{km}$. It is always assumed that d_{km} is known (without loss of generality $d_{km} = 0, k = 1, \cdots, K, m = 1, \cdots, M$). Otherwise, even in the case of correct detection, it is not possible to know the index of the corresponding symbol; meaning that communication is not possible. In addition, in most of the work in the literature, symbol level synchrony is assumed, i.e., $\tau_{km} = 0,\ k = 1, \cdots, K, m = 1, \cdots, M$ which might be challenging, especially, in a multiuser scenario where users are located at various places experiencing completely different paths. Even if we have perfect control over the delays at transmitters, we can use such a control to synchronize the signals at one of the receivers. Then, in a multi-user system with several receivers, it is impossible to have perfect time-synchronization at the symbol level for all receivers. In addition, even knowing/estimating the values of the time asynchrony, i.e., τ_{km} values, may not be possible for more than a few number of receive antennas. Therefore, we consider the general case in which the time delays are treated as random variables. Usually, due to the lack of information about time delays, the time delays are assumed to have uniform distribution. However, this assumption hides the fact that one of the signals arrives at the receiver first and provides the time origin for performing matched filtering and sampling processes. To explain it further, assume that we have two users. Each user's signal is received first with probability of half. Therefore, each user will have zero timing mismatch with probability of half and uniform timing mismatch between $(0, T_s)$ otherwise. Hence, the most

general assumption for the distribution of time delays is that each of them is chosen from the following distribution:

$$f(\tau) = \frac{1}{K}\bar{\delta}(\tau) + \frac{K-1}{K}U(0, T_s) \tag{3}$$

where $\bar{\delta}(.)$ is the continuous Delta function and $U(0, T_s)$ is the uniform function in the interval of $(0, T_s)$. This distribution shows that with probability of $\frac{1}{K}$, each user signal is received before other users' signals, i.e. $\tau_{km} = 0$, and with the probability of $\frac{K-1}{K}$, it is uniformly distributed in the interval of $(0, T_s)$. From now on, we assume d_{km} is equal to zero and τ_{km} is a random variable following the density function in Eq. (3). Note that our approach and analysis works for any other known density function as well.

III. Receiver Design

In this section, we explain the receiver design that includes the transformation of the continuous signal in Eq. (2) into discrete samples and the combination of the obtained samples at different receive antennas by the MRC method.

A. Output Samples

To obtain the discrete samples of the received signal, first the continuous received signal should be passed through a matched filter and its output can be written as follows:

$$\hat{\psi}_m(t) = \sqrt{\rho_d}\sum_{k=1}^{K}\sqrt{\beta_k}h_{km}\sum_{i=1}^{N}b_k(i)g(t-(i-1)T_s-\tau_{km}) + \nu_m(t) * p(t) \tag{4}$$

where $g(t) = p(t) * p(t)$. The convolution $g(t)$, called convoluted pulse shape is zero outside the interval of $[0 \quad 2T]$. The sampling instants are represented as t_n^s and are equal to $e + T + (n-1)T_s, n = 1, \cdots, N$. The quantity of e is a design parameter that affects the performance significantly. Optimizing sampling instants can be translated into optimizing the factor e that is defined as the sampling origin. If all the received signals were synchronized, then $e = 0$ would be the optimum value, which is the assumption in most of the work in the literature. However, due to having unknown delays among received signals, the optimum value of e is not zero anymore and will be found based on the system model characteristics. The obtained samples at the sampler of the mth receive antenna denoted by $y_m(n) = \hat{\psi}_m(t)|_{t_n^s}$ can be written as:

$$y_m(n) = \sqrt{\rho_d}\sum_{k=1}^{K}\sqrt{\beta_k}h_{km}\sum_{i=1}^{N}b_k(i)g(e+T+(n-i)T_s-\tau_{km}) + \hat{\nu}_m(t)|_{e+T+(n-1)T_s} \tag{5}$$

where $\hat{\nu}_m(t) = \nu_m(t) * p(t)$. Eq. (5) can also be interpreted as passing the $T+e$ shifted version of the output of the matched filter through a sampler with sampling frequency of $f_s = \frac{1}{T_s}$. After obtaining N samples, we can put them together and form the system model equation as follows:

$$\boldsymbol{y_m} = \sqrt{\rho_d} \sum_{k=1}^{K} \sqrt{\beta_k} h_{km} \boldsymbol{G_{km}} \boldsymbol{b_k} + \boldsymbol{n_m} \quad 1 \leq l \leq K,\ 1 \leq m \leq M \tag{6}$$

where $\boldsymbol{b_k} = [b_k(1), b_k(2), \cdots, b_k(N)]^T$ is the transmitted frame by the kth user and $\boldsymbol{n_m} = [n_m(1), n_m(2), \cdots, n_m(N)]^T$ is the noise vector containing samples of $\hat{\nu}_m(t)$, i.e., $n_m(n) = \hat{\nu}_m(t)|_{e+T+(n-1)T_s}, 1 \leq n \leq N$. Also, $\boldsymbol{G_{km}}$ is an $N \times N$ matrix defined as:

$$\boldsymbol{G_{km}} = \begin{pmatrix} g(e+T-\tau_{km}) & \cdots & g(e+T+(1-N)T_s-\tau_{km}) \\ g(e+T+T_s-\tau_{km}) & \cdots & g(e+T+(2-N)T_s-\tau_{km}) \\ \vdots & \ddots & \vdots \\ g(e+T+(N-1)T_s-\tau_{km}) & \cdots & g(e+T-\tau_{km}) \end{pmatrix}_{N\times N} \tag{7}$$

Defining $\boldsymbol{T_{km}} = \sqrt{\beta_k} h_{km} \boldsymbol{G_{km}}$, Eq. (6) can be written as the following short form:

$$\boldsymbol{y_m} = \sqrt{\rho_d} \sum_{k=1}^{K} \boldsymbol{T_{km}} \boldsymbol{b_k} + \boldsymbol{n_m} \quad 1 \leq k \leq K,\ 1 \leq m \leq M \tag{8}$$

The noise vector has zero mean and identity covariance matrix.

B. Maximum Ratio Combining

As a quick recap, the MRC is a low complexity receiver that consists of multiplying samples of each receive antenna by conjugate of the corresponding channel coefficient estimate and then averaging them among all the receive antennas. These estimates are usually obtained by transmitting pilot sequences at the beginning of the frame. Then, those estimated channel coefficients are used to perform MRC. Denoting $\tilde{c}_{lm}$ as the estimate of the channel coefficient between the lth user and the mth receive antenna, the MRC output for detection of the lth user's symbols, i.e, $\boldsymbol{y_l^{mrc}} = \frac{1}{M} \sum_{m=1}^{M} \tilde{c}_{lm}^* \boldsymbol{y_m}$, can be expressed as:

$$\boldsymbol{y_l^{mrc}} = \sqrt{\rho_d} \sum_{k=1}^{K} \boldsymbol{T_{lk}^{mrc}} \boldsymbol{b_k} + \boldsymbol{n_l^{mrc}} \tag{9}$$

where the effective channel matrices and the resulting noise vector are denoted by $\boldsymbol{T_{lk}^{mrc}}$ and $\boldsymbol{n_l^{mrc}}$, and will be defined later based on available CSI and detection methods. In the next section, we analyze the performance of the MRC detection for perfect CSI and estimated CSI at the receiver. First, to reveal the main effects of the interuser time delays, we consider the case

that channel coefficients are perfectly known at the receiver, i.e, $\tilde{c}_{lm} = c_{lm}, l = 1, \cdots, K, m = 1, \cdots, M$. Next, we consider the more general case where the channel coefficients are estimated by sending pilot sequences.

IV. Analysis of Achievable Rates

A. Perfect CSI

In this section, we assume that channel coefficients are estimated separately for each user. It might be impractical due to the large number of users being served by the base station; however, it will uncover the main effects of unknown time delays on the performance. Unlike the case of perfect synchronization where there is no uncertainty in the effective channel coefficients, here, the effective channel matrices consist of random variables which only their statistics are known by the receiver. The source of randomness is the unknown delays between received signals. By assuming $\tilde{c}_{km} = c_{km}$, the random matrix $\boldsymbol{T}_{\boldsymbol{lk,p}}^{\boldsymbol{mrc}}$ can be represented as follows:[1]

$$\boldsymbol{T}_{\boldsymbol{lk,p}}^{\boldsymbol{mrc}} = \frac{1}{M} \sum_{m=1}^{M} \sqrt{\beta_l \beta_k} h_{lm}^* h_{km} \boldsymbol{G}_{\boldsymbol{km}} \tag{10}$$

With the assumption of symbol level synchronization between received signals of different users, $\boldsymbol{T}_{\boldsymbol{lk,p}}^{\boldsymbol{mrc}}$ turns into $\frac{1}{M} \sum_{m=1}^{M} \sqrt{\beta_l \beta_k} h_{lm}^* h_{km} \boldsymbol{I}_{\boldsymbol{N}}$, which means that there is no ISI. As a result, the major impairment comes from interuser interference and it is shown in [24] that the approximate achievable rate can be calculated as:

$$R_{l,p}^{mrc-ideal} \approx \log_2 \left(1 + \frac{\rho_d \beta_l (M+1)}{\rho_d \sum\limits_{\substack{k=1 \\ k \neq l}}^{K} \beta_k + 1} \right) \tag{11}$$

However, due to the existence of unwanted mismatch between received signals, this ideal rate is not achievable by the MRC receiver. In fact, by overlooking the symbol level synchronization, the major impairment would be ISI and the achievable rate is denoted in the next theorem.

[1]The subscripts p and ip are used for perfect CSI and imperfect CSI, respectively.

Theorem 1: The achievable rate of the MRC receiver for User l, when there is unknown time delays between received signals, can be approximated as:

$$R_{l,p}^{mrc} \approx \log_2 \left(1 + \frac{\rho_d \beta_l (2E[g_0^2] + (M-1)E[g_0]^2)}{\rho_d \sum\limits_{i=-I}^{I} E[g_i^2] \sum\limits_{\substack{k=1 \\ k \neq l}}^{K} \beta_k + \rho_d \beta_l \sum\limits_{\substack{i=-I \\ i \neq 0}}^{I} (2E[g_i^2] + (M-1)E[g_i]^2) + 1} \right) \tag{12}$$

where

$$E[g_i^n] = \int_{-\infty}^{\infty} g^n (e + T + iT_s - \tau) f(\tau) d\tau \tag{13}$$

and I is the number of significant adjacent side lobes of the pulse shape.

Proof: the proof is presented in Appendix A. ■

The first term in the denominator of Eq. (12) is IUI caused by other users. However, its difference with Eq. (11) is that due to unknown timing mismatch values the aforementioned IUI is not only caused by the same indexed symbols but also the adjacent symbols, represented by multiplication factor of $\sum_{i=-I}^{I} E[g_i^2]$ in Eq. (12). The second term in the denominator is the ISI, which is caused by adjacent symbols of the desired user. By increasing M, the effect of ISI is much more severe than IUI. The last term is related to additive white noise.

Example 1: For the ideal case of perfect synchronization, i.e, $f(\tau) = \bar{\delta}(\tau)$ Eq. (12) turns into:

$$R_{l,p}^{mrc} \approx \log_2 \left(1 + \frac{g^2(e+T)\rho_d \beta_l (M+1)}{g^2(e+T)\rho_d \sum\limits_{\substack{k=1 \\ k \neq l}}^{K} \beta_k + \rho_d \left(\sum\limits_{\substack{i=-I \\ I \neq 0}}^{I} g^2(e + T + iT_s) \right) (\sum\limits_{\substack{k=1 \\ k \neq l}}^{K} \beta_k + (M+1)\beta_l) + 1} \right) \tag{14}$$

Now, it is clear that if the pulse shape satisfies the Nyquist no-ISI condition, by putting $e = 0$, i.e., sampling at $T + nT_s$ instants, the second term in the denominator can be completely eliminated and Eq. (14) turns into Eq. (11). Therefore, the formula in Eq. (12) is general and covers all sorts of delay distributions and pulse shapes including the ideal case of symbol-level synchronization.

Example 2: We assume that rectangular pulse shape is used and time delays follow the distribution in Eq. (3). Then, values of $E[g_i]$ and $E[g_i^2]$ are calculated as follows:

$$\left\{\begin{array}{c} E[g_0]=\frac{1}{K}\left(1-\frac{e}{T}\right)+\frac{K-1}{K}\left(\frac{T^2-2e^2+2eT}{2T^2}\right) \\ E[g_{-1}]=\frac{1}{K}\left(\frac{e}{T}\right)+\frac{K-1}{K}\left(\frac{e^2}{2T^2}\right) \\ E[g_1]=\frac{K-1}{K}\left(\frac{(T-e)^2}{2T^2}\right) \end{array}\right\}, \left\{\begin{array}{c} E[g_0^2]=\frac{1}{K}\left(1-\frac{e}{T}\right)^2+\frac{K-1}{K}\left(\frac{1}{3}+\frac{e}{T}-\frac{e^2}{T^2}\right) \\ E[g_{-1}^2]=\frac{1}{K}\left(\frac{e}{T}\right)^2+\frac{K-1}{K}\left(\frac{e^3}{3T^3}\right) \\ E[g_1^2]=\frac{K-1}{K}\left(\frac{(T-e)^3}{3T^3}\right) \end{array}\right\}$$

Note that for the rectangular pulse shape, $E[g_i]$ and $E[g_i^2]$ are nonzero only when $i=-1,0,1$. Assume that $K=10$, then, based on the choice of e, an approximate expression for the achievable rate can be calculated. For example, by inserting $e=0$, the approximate achievable rate is:

$$R_{l,p}^{mrc}\approx\log_2\left(1+\frac{\rho_d\beta_l(0.8+0.3(M-1))}{0.7\rho_d\sum\limits_{\substack{k=1\\k\neq l}}^{K}\beta_k+\rho_d\beta_l(0.6+0.2(M-1))+1}\right) \tag{15}$$

If we choose $e=0.5$, the approximate achievable rate is:

$$R_{l,p}^{mrc}\approx\log_2\left(1+\frac{\rho_d\beta_l(1.1+0.5(M-1))}{0.6\rho_d\sum\limits_{\substack{k=1\\k\neq l}}^{K}\beta_k+\rho_d\beta_l(0.2+0.04(M-1))+1}\right) \tag{16}$$

Therefore, for large M, $e=0.5$ results in better performance compared to $e=0$.

In the ideal case of synchronized reception, the power scale law of massive MIMO systems states that the transmit power of each user can be cut down by $\frac{1}{M}$ with no degradation in the achievable rate of each user, i.e., $R_{l,p}^{ideal}\rightarrow\log_2(1+E_d\beta_l)\ as\ M\rightarrow\infty, \rho_d=\frac{E_d}{M}$ [17]. However, by ignoring the inevitable timing mismatch, the promised benefit of power scaling in massive MIMO setting vanishes. In more detail, if we put $\rho_d=\frac{E_d}{M}$ in Eq. (12) and let M go to infinity, then we have:

$$R_{l,p}^{mrc}\rightarrow\log_2\left(1+\frac{E_d\beta_l E[g_0]^2}{E_d\beta_l\sum\limits_{\substack{i=-I\\i\neq 0}}^{I}E[g_i]^2+1}\right) \tag{17}$$

The achievable rate in Eq. (17) is limited by ISI, and by increasing the transmit power it will be saturated to a constant value, i.e.:

$$R_{l,p}^{mrc} \to \log_2 \left(1 + \frac{E[g_0]^2}{\sum\limits_{\substack{i=-I \\ i\neq 0}}^{I} E[g_i]^2} \right) \tag{18}$$

Therefore, at high SNR regime, no matter how much transmit power is used, the achievable rate converges to a fixed value independent of the transmit power. This fixed value depends on the delay distribution, pulse shape and sampling origin e. Using this criterion, more robust pulse shapes can be designed to make the performance less vulnerable to unknown time delays. Designing suitable pulse shapes is out of the scope of this work; however, for any given pulse shape, the sampling origin can be optimized. For example, the optimum value of e for rectangular pulse shape and delay distribution presented in Eq. (3) can be found by optimizing the following expression which is obtained by inserting the values of $E[g_i]$ into Eq. (18):

$$\max_{e} \frac{(2(T^2 - eT) + (K-1)(T^2 - 2e^2 + 2eT))^2}{(2eT + (K-1)e^2)^2 + (K-1)^2(T-e)^4} \tag{19}$$

The above optimization problem can be solved to obtain the optimal value of e for any number of users. The optimal values of e for $T = 1$ and a few examples of K are shown in Table I. By

TABLE I: Optimal Sampling Origin e

Case	K=2	K=4	K=6	K=8	K=10	K=12	K=14	K=16
Optimal e	0.18	0.35	0.41	0.44	0.45	0.46	0.46	0.47

increasing the number of users, the optimal value of e approaches half. The simulation results on the optimal values of e for the root raised cosine pulse shape are shown in Section V.

B. Imperfect CSI

In practice, acquiring CSI is not free. In fact, the channel coefficients are estimated by sending known sequences of symbols, called pilot sequences, and costs a portion of the coherent time T_c. We assume that each user assigns its first N_p symbols of each frame to send pilot symbols. We denote the assigned pilot sequence to the kth user as $\boldsymbol{p_k} = [p_k(1), \cdots, p_k(N_p)]$. It is common in the literature that the assigned pilot sequences for different users are mutually orthogonal, i.e.,

$\langle \boldsymbol{p_i}.\boldsymbol{p_j} \rangle = \delta(i-j)$, where $\langle \ . \ \rangle$ shows the inner product. In addition, N_p should be equal to or greater than the number of users and its optimal value is shown to be $N_p = K$ [25]. The mutual orthogonality enables all the users to send the pilot symbols simultaneously without interfering with each other. The $K \times N_p$ matrix that contains all the pilot sequences is represented by:

$$\boldsymbol{\Phi} = \begin{pmatrix} p_1(1) & \cdots & p_1(N_p) \\ p_2(1) & \cdots & p_2(N_p) \\ \vdots & \ddots & \vdots \\ p_K(1) & \cdots & p_K(N_p) \end{pmatrix}_{K \times N_p} \tag{20}$$

Due to orthogonality between rows, the pilot matrix is unitary, i.e., $\boldsymbol{\Phi}\boldsymbol{\Phi}^H = \boldsymbol{I_K}$. In the ideal case of perfect synchronization, the received signal can be written as:

$$\boldsymbol{Y_p} = \sqrt{\rho_p}\boldsymbol{C}\boldsymbol{\Phi} + \boldsymbol{N} \tag{21}$$

where $\boldsymbol{Y_p}$ and $\boldsymbol{N}$ are $M \times N_p$ matrices of received samples and noise samples, respectively, and $\boldsymbol{C}$ is equal to $\boldsymbol{H}\boldsymbol{D}^{1/2}$ where $\boldsymbol{H}$ is the $M \times K$ matrix of fading coefficients between the K users and the BS, i.e., $\boldsymbol{H}(k,m) = h_{km}$, and $\boldsymbol{D}$ is a $K \times K$ diagonal matrix containing the path-loss coefficients, i.e., $\boldsymbol{D}(k,k) = \beta_k$. Also, ρ_p is the power assigned to transmission of pilot sequences and it is equal to $\rho_p = N_p\rho_d$. Therefore, the least square estimate of the channel matrix $\boldsymbol{C}$ can be calculated as:

$$\tilde{\boldsymbol{C}} = \frac{1}{\sqrt{\rho_p}}\boldsymbol{Y_p}\boldsymbol{\Phi}^H \tag{22}$$

Then, $\tilde{\boldsymbol{C}}$ is used to perform MRC. The achievable rate by each user is equal to [17]:

$$R_{l,ip}^{ideal} \approx \log_2\left(1 + \frac{N_p\rho_d^2\beta_l^2(M+1)}{\rho_d(N_p\rho_d\beta_l+1)\sum\limits_{\substack{k=1 \\ k\neq l}}^{K}\beta_k + \rho_d(N_p+1)\beta_l + 1}\right) \tag{23}$$

Eq. (23) shows that the effect of reduction in the power of pilot and data symbols are multiplied together and as a result, the power-scaling law admits a power reduction in the order of $\frac{1}{\sqrt{M}}$ with no degradation in the achievable rate of each user, i,e., $\bar{R}_{l,ip}^{ideal} \rightarrow \log_2(1 + N_pE_d^2\beta_l^2) \ as \ M \rightarrow \infty, \rho_d = \frac{E_d}{\sqrt{M}}$. [17]. However, due to the existence of unknown time delays, the estimation process is also degraded and as a result, the channel estimations are contaminated by unwanted channel coefficients. This phenomenon is similar to the "pilot contamination" effect in which channel estimates are contaminated due to the pilot reuse. As a result, not only ISI but also IUI

will degrade the performance. In what follows, we provide a similar analysis for the channel estimation when the misalignment exists between received signals. Time delays modify Eq. (21) to:

$$\boldsymbol{Y_p} = \sqrt{\rho_p} \sum_{i=-I}^{i=I} \boldsymbol{C^i \Phi^i} + \boldsymbol{N} \tag{24}$$

where $\boldsymbol{C^i}_{M\times K}$ and $\boldsymbol{\Phi^i}_{K\times N_p}$ are defined as follows:

$$\boldsymbol{C^i} = \begin{pmatrix} g(e+T+iT_s-\tau_{11})\sqrt{\beta_1}h_{11} & \cdots & g(e+T+iT_s-\tau_{K1})\sqrt{\beta_K}h_{K1} \\ g(e+T+iT_s-\tau_{12})\sqrt{\beta_1}h_{12} & \cdots & g(e+T+iT_s-\tau_{K2})\sqrt{\beta_K}h_{K2} \\ \vdots & \ddots & \vdots \\ g(e+T+iT_s-\tau_{1M})\sqrt{\beta_1}h_{1M} & \cdots & g(e+T+iT_s-\tau_{KM})\sqrt{\beta_K}h_{KM} \end{pmatrix}$$

$$\boldsymbol{\Phi^{i\leq 0}} = \begin{pmatrix} p_1(1-i) & \cdots & p_1(N_p) & 0 & \cdots & 0 \\ p_2(1-i) & \cdots & p_2(N_p) & 0 & \cdots & 0 \\ \vdots & \ddots & \vdots & & & \\ p_K(1-i) & \cdots & p_K(N_p) & 0 & \cdots & 0 \end{pmatrix}, \boldsymbol{\Phi^{i\geq 0}} = \begin{pmatrix} 0 & \cdots & 0 & p_1(1) & \cdots & p_1(N_p-i) \\ 0 & \cdots & 0 & p_2(1) & \cdots & p_2(N_p-i) \\ \vdots & \ddots & \vdots & & & \\ 0 & \cdots & 0 & p_K(1) & \cdots & p_K(N_p-i) \end{pmatrix}$$

The process of de-spreading, which is multiplying the received pilot signal by $\frac{1}{\sqrt{\rho_p}}\boldsymbol{\Phi}^H$, yields the following channel matrix estimator:

$$\tilde{\boldsymbol{C}} = \boldsymbol{C^0} + \sum_{\substack{i=-I \\ i\neq 0}}^{i=I} \boldsymbol{C^i \Phi^i \Phi}^H + \tilde{\boldsymbol{N}} \tag{25}$$

where $\tilde{\boldsymbol{N}}$ is the estimation noise. We denote $\boldsymbol{\Phi^i \Phi}^H$ by $\boldsymbol{\Upsilon^i}$ which is equal to $\boldsymbol{I_K}$ for $i = 0$, and for the other values of i can be calculated as:

$$(\boldsymbol{\Upsilon^{i<0}})^T = \boldsymbol{\Upsilon^{i>0}} = \begin{pmatrix} \langle\, \boldsymbol{p_1}(1:N_p-i).\boldsymbol{p_1}(1+i:N_p)\rangle & \cdots & \langle\, \boldsymbol{p_1}(1:N_p-i).\boldsymbol{p_K}(1+i:N_p)\rangle \\ \vdots & \ddots & \vdots \\ \langle\, \boldsymbol{p_K}(1:N_p-i).\boldsymbol{p_1}(1+i:N_p)\rangle & \cdots & \langle\, \boldsymbol{p_K}(1:N_p-i).\boldsymbol{p_K}(1+i:N_p)\rangle \end{pmatrix}$$

where $\boldsymbol{p}(i:j)$ represents the vector $[p(i), p(i+1), \cdots, p(j)]$. Therefore, the channel coefficient estimate of User l to receive antenna m can be represented as:

$$\tilde{c}_{lm} = g(e+T-\tau_{lm})c_{lm} + \sum_{\substack{i=-I \\ i\neq 0}}^{i=I} g(e+T+iT_s-\tau_{lm})\boldsymbol{\Upsilon^i}(l.l)c_{lm} + \sum_{\substack{j=1 \\ j\neq l}}^{K} \lambda_{ljm}c_{jm} + \tilde{n}_{lm} \tag{26}$$

where λ_{ljm} is called "the leakage factor" from User j to the estimation of the User l's channel coefficient to receive antenna m and is equal to:

$$\lambda_{ljm} = \sum_{i=-I}^{i=I} g(e + T + iT_s - \tau_{jm}) \boldsymbol{\Upsilon^i}(j, l) \tag{27}$$

Besides the estimation noise, unknown time delays impose three additional impurities to the channel estimation. The first one is due to imperfect sampling time whose effect is shown by the multiplication factor of $g(e + T - \tau_{km})$. The second impurity in Eq. (26) originates from adjacent interfering symbols of the desired user. The last impurity is similar to the "pilot contamination" effect, i.e., the channel estimation of each user to the mth receive antenna is contaminated by channel coefficients of other users. In the "pilot contamination" problem, the reason of contamination is reusing the same pilot sequences in different cells, however, here the reason is unknown timing mismatches between received signals. Due to the time asynchrony between received signals, the orthogonality between pilot sequences is not preserved anymore and the de-spreading matrix is not able to eliminate the effect of interfering users. When the perfect synchronization is assumed, $\boldsymbol{\Upsilon^i}$ is all zero matrix for all values of i except $\boldsymbol{\Upsilon^0}$ which is equal to $\boldsymbol{I_K}$. In this case, the leakage factors will be equal to zero and by choosing $e = 0$, the set-up will be identical to that of the perfect synchronization, i.e., $\tilde{c}_{lm} = c_{lm} + \tilde{n}_{lm}$.

By using the channel estimates of (26) for performing MRC, we can calculate the effective channel matrices as:

$$\boldsymbol{T^{mrc}_{lk,ip}} = \frac{1}{M} \sum_{m=1}^{M} \sum_{j=1}^{K} \lambda_{ljm} \sqrt{\beta_j \beta_k} h^*_{jm} h_{km} \boldsymbol{G_{km}} \tag{28}$$

The effective noise vector is also equal to:

$$\boldsymbol{n^{mrc}_{l,ip}} = \frac{\sqrt{\rho_d}}{M} \sum_{m=1}^{M} \tilde{n}^*_{lm} \sum_{k=1}^{K} \sqrt{\beta_k} h_{km} \boldsymbol{G_{km}} \boldsymbol{b_k} + \frac{1}{M} \sum_{m=1}^{M} \left(\sum_{j=1}^{K} \lambda_{ljm} \sqrt{\beta_j} h^*_{jm} + \tilde{n}^*_{lm} \right) \boldsymbol{n_m} \tag{29}$$

Then, the achievable rates for imperfect channel state information, is presented in the next theorem.

Theorem 2: The achievable rate by the MRC receiver using orthogonal channel estimation, when there is unknown time delays between received signals can be approximated as follows:

$$R^{mrc}_{l,ip} \approx \log_2 \left(1 + \frac{desired\ signal}{IUI + ISI + noise} \right) \tag{30}$$

where desired signal, ISI, IUI and noise components are defined as follows, respectively:

$$desired\ signal = \rho_d \beta_l^2 (2\gamma''_{lll}(0) + (M-1)(\gamma'_{lll}(0))^2)) + \rho_d \beta_l \sum_{\substack{j=1 \\ j\neq l}}^{K} \beta_j \gamma''_{ljl}(0)$$

$$ISI = \rho_d \beta_l^2 \sum_{\substack{n=-I \\ n\neq 0}}^{I} (2\gamma''_{lll}(n) + (M-1)(\gamma'_{lll}(n))^2) + \rho_d \beta_l \sum_{\substack{j=1 \\ j\neq l}}^{K} \beta_j \sum_{\substack{n=-I \\ n\neq 0}}^{I} \gamma''_{ljl}(n)$$

$$IUI = \rho_d \sum_{\substack{k=1 \\ k\neq l}}^{K} \beta_k^2 \sum_{n=-I}^{I} (2\gamma''_{lkk}(n) + (M-1)(\gamma'_{lkk}(n))^2) + \rho_d \sum_{\substack{k=1 \\ k\neq l}}^{K} \sum_{\substack{j=1 \\ j\neq k}}^{K} \beta_k \beta_j \sum_{n=-I}^{I} \gamma''_{ljk}(n)$$

$$noise = \frac{\rho_d}{\rho_p} \sum_{k=1}^{K} \beta_k \sum_{n=-I}^{I} E[g_n^2] + \sum_{k=1}^{K} \beta_k \lambda''_{lk} + \frac{1}{\rho_p}$$

where

$$\begin{aligned}
\gamma'_{ljk}(n) &= E[\gamma_{ljkm}(n)] \\
&= E[\lambda_{ljm} g(e + T + nT_s - \tau_{km})]] \\
&= \int_{-\infty}^{\infty} \int_{-\infty}^{\infty} \left(\sum_{i=-I}^{i=I} \boldsymbol{\Upsilon}^{\boldsymbol{i}}(j,l) g(e + T + iT_s - \tau_j) \right) g(e + T + nT_s - \tau_k) f(\tau_j) f(\tau_k) d\tau_j d\tau_k
\end{aligned}$$

Note that after taking average over all receive antennas, the receive antenna index is discarded. The terms $\gamma''_{ljk}(n)$ and λ''_{lk} are defined similarly as:

$$\gamma''_{ljk}(n) = \int_{-\infty}^{\infty} \int_{-\infty}^{\infty} \left(\sum_{i=-I}^{i=I} \boldsymbol{\Upsilon}^{\boldsymbol{i}}(j,l) g(e + T + iT_s - \tau_j) \right)^2 g^2(e + T + nT_s - \tau_k) f(\tau_j) f(\tau_k) d\tau_j d\tau_k$$

and

$$\lambda''_{lk} = E[\lambda_{lkm}^2] = \int_{-\infty}^{\infty} \left(\sum_{i=-I}^{i=I} \boldsymbol{\Upsilon}^{\boldsymbol{i}}(k,l) g(e + T + iT_s - \tau) \right)^2 f(\tau_k) d\tau_k$$

Proof: the proof is presented in Appendix B. ■

These results are general for any pilot matrices and delay distributions. Values of $\gamma'_{ljk}(n), \gamma''_{ljk}(n), \lambda''_{lk}$ and $E[g_n^2]$ only depend on the pulse shape, pilot sequences and the delay distribution which can be calculated analytically or numerically. Similar to Example 1, we can show that by inserting $f(\tau) = \bar{\delta}(\tau)$ and $e = 0$, Eq. (30) simplifies to Eq. (23) which shows that the perfect synchronized scenario is a special example of the general formula in Theorem 2.

Example 3: We consider another simple example to clarify Theorem 2. Assume that the pulse shape is rectangular, $K = 2$ and $\boldsymbol{I_2}$ is used as the pilot matrix. Then,

$$\boldsymbol{\Upsilon^0} = \boldsymbol{I_2}, \quad \boldsymbol{\Upsilon^{-1}} = \begin{bmatrix} 0 & 0 \\ 1 & 0 \end{bmatrix}, \quad \boldsymbol{\Upsilon^1} = \begin{bmatrix} 0 & 1 \\ 0 & 0 \end{bmatrix} \tag{31}$$

Hence, the "leakage factors" , i.e., λ_{11m} and λ_{12m} are equal to $g(e+T-\tau_{1m})$ and $g(e-\tau_{2m})$, respectively. The values of λ''_{1k} are expected values of λ^2_{1km} with respect to τ_{km}, therefore we have:

$$\lambda''_{11} = \frac{1}{2}\left(1-\frac{e}{T}\right)^2 + \frac{1}{2}\left(\frac{1}{3}+\frac{e}{T}-\frac{e^2}{T^2}\right), \quad \lambda''_{12} = \frac{e^2}{2T^2}\left(1+\frac{e}{3T}\right) \tag{32}$$

The values of $\gamma'_{1jk}(n)$ are aslo expected values of $\lambda_{1jm}g(e+T+nT-\tau_{km})$ with respect to τ_{jm} and τ_{km}. As a result, we have, $\gamma'_{111}(n) = E[g(e+T-\tau_{1m})g(e+T+nT-\tau_{1m})]$, $\gamma'_{112}(n) = E[g(e+T-\tau_{1m})]E[g(e+T+nT-\tau_{2m})]$, $\gamma'_{121}(n) = E[g(e-\tau_{2m})]E[g(e+T+nT-\tau_{1m})]$ and $\gamma'_{122}(n) = E[g(e-\tau_{2m})g(e+T+nT-\tau_{2m})]$. After some calculations, we will have:

$$\left\{\begin{array}{c} \gamma'_{111}(0) = \frac{1}{2}(1-\frac{e}{T})^2 + \frac{1}{2}(\frac{1}{3}+\frac{e}{T}-\frac{e^2}{T^2}) \\ \gamma'_{111}(-1) = \frac{1}{2}(\frac{e}{T}-\frac{e^2}{2T^2}-\frac{e^3}{3T^3}) \\ \gamma'_{111}(1) = \frac{(T-e)^2}{2T^2}-\frac{(T-e)^3}{3T^3} \end{array}\right\}, \quad \left\{\begin{array}{c} \gamma'_{112}(0) = \frac{1}{4}(\frac{3T^2-2e^2}{2T^2})^2 \\ \gamma'_{112}(-1) = \frac{1}{4}(\frac{3T^2-2e^2}{2T^2})(\frac{2eT+e^2}{2T^2}) \\ \gamma'_{112}(1) = \frac{1}{4}(\frac{3T^2-2e^2}{2T^2})\frac{(T-e)^2}{2T^2} \end{array}\right\} \tag{33}$$

$$\left\{\begin{array}{c} \gamma'_{121}(0) = \frac{1}{4}(\frac{2eT+e^2}{2T^2})(\frac{3T^2-2e^2}{2T^2}) \\ \gamma'_{121}(-1) = \frac{1}{4}(\frac{2eT+e^2}{2T^2})^2 \\ \gamma'_{121}(1) = \frac{1}{4}(\frac{2eT+e^2}{2T^2})\frac{(T-e)^2}{2T^2} \end{array}\right\}, \quad \left\{\begin{array}{c} \gamma'_{122}(0) = \frac{1}{2}(\frac{e}{T}-\frac{e^2}{2T^2}-\frac{e^3}{3T^3}) \\ \gamma'_{122}(-1) = \frac{e^2}{2T^2}(1+\frac{e}{3T}) \\ \gamma'_{122}(1) = 0 \end{array}\right\} \tag{34}$$

Values of $\gamma''_{1kj}(n)$ can be calculated similarly. Then, based on the choice of e, approximate expressions for achievable rates can be found. For example, by inserting $e = 0$, the approximate achievable rates are:

$$R^{mrc}_{1,ip} \approx \log_2\left(1+\frac{\rho_d\beta_1^2(1.2+0.4(M-1))}{\rho_d\beta_1^2(0.08)^2(M-1)+0.5\rho_d\beta_1\beta_2+0.8\frac{\rho_d}{\rho_p}\sum_{k=1}^{2}\beta_k+0.7\beta_1+\frac{1}{\rho_p}}\right)$$

If we choose $e = 0.5$, the approximate achievable rates will be:

$$R^{mrc}_{1,ip} \approx$$

$$\log_2\left(1+\frac{\rho_d\beta_1^2(0.5+0.2(M-1))}{\left(\rho_d\beta_1^2(0.2)^2+\rho_d\beta_2^2(0.3)^2\right)(M-1)+0.25\rho_d\beta_1\beta_2+0.5\frac{\rho_d}{\rho_p}\sum_{k=1}^{2}\beta_k+0.4\beta_1+0.2\beta_2+\frac{1}{\rho_p}}\right)$$

Therefore, for large M, $e = 0$ results in better performance compared to $e = 0.5$. However, when the number of users increases the optimum value of e changes.

Note that due to the existence of timing mismatch, the promised power scaling law is demolished. If we reduce the transmit power by order of $\frac{1}{\sqrt{M}}$ and let M go to infinity, then the achievable rate for each user is:

$$R_{l,ip}^{mrc} \to \log_2 \left(1 + \frac{N_p E_d^2 \beta_l^2 (\gamma'_{ll}(0))^2}{N_p E_d^2 \beta_l^2 \sum\limits_{\substack{i=-I \\ i\neq 0}}^{i=I} (\gamma'_{ll}(i))^2 + N_p E_d^2 \sum\limits_{\substack{k=1 \\ k\neq l}}^{K} \beta_k^2 \sum\limits_{i=-I}^{i=I} (\gamma'_{lkk}(i))^2 + 1} \right) \tag{35}$$

By increasing the transmit power, the achievable rate saturates at the following fixed value:

$$R_{l,ip}^{mrc} \to \log_2 \left(1 + \frac{\beta_l^2 (\gamma'_{ll}(0))^2}{\beta_l^2 \sum\limits_{\substack{i=-I \\ i\neq 0}}^{i=I} (\gamma'_{ll}(i))^2 + \sum\limits_{\substack{k=1 \\ k\neq l}}^{K} \beta_k^2 \sum\limits_{i=-I}^{i=I} (\gamma'_{lkk}(i))^2} \right) \tag{36}$$

The above analysis shows that, the promised single user bound is degraded by ISI and IUI due to imperfect channel estimation. When we had perfect information of channel coefficients, the only degradation was ISI due to timing mismatch, however, by using orthogonal sequences to estimate the channel coefficients IUI is also another source of degradation. For any given pulse shape and time delay, the performance criteria in Eq. (36) can be optimized by changing the sampling origin e. For example, the optimum value of e for rectangular pulse shape and the delay distribution presented in Eq. (3), is shown in Table II. Again, as K increases, the optimal

TABLE II: Optimal Sampling Origin e

Case	K=2	K=4	K=6	K=8	K=10	K=12	K=14	K=16
Optimal e	0	0.12	0.28	0.38	0.44	0.46	0.46	0.48

value of e approaches half. While such an optimization can increase the achievable rates in Theorems 1 and 2, many promising benefits of using a massive number of receive antennas will still be out of reach in the presence of unknown time delays. Therefore, we design two receiver structures, for perfect CSI and imperfect CSI scenarios, to remove the unwanted effects of ISI and IUI imposed by unknown time delays. The details are presented next.

C. MRC-ZF Receiver Structure

In an ideal massive MIMO system, the achievable uplink rate grows unbounded when M grows large. Therefore, we can scale down the power of each user by the ratios of M and $\sqrt{M}$ for perfect and imperfect CSI, respectively, to achieve the single user performance. However, in a realistic massive MIMO system where timing mismatch among received signals is inevitable, the uplink achievable rate using the MRC receiver approaches a constant value when M grows large, as shown in Theorems 1 and 2. Therefore, the power scaling law provided by the MRC receiver in a perfectly synchronized massive MIMO system is not achievable with unknown time delays. Hence, we modify the MRC receiver to cancel the effects of ISI and IUI imposed by unknown time delays.

When channel coefficients are estimated one by one with no error, the dominant degradation is ISI. On the other hand, when the channel coefficients are estimated simultaneously by sending pilot sequences, the degradation is caused by ISI and IUI. The underlying reason is the expected value of effective channel matrices, $\boldsymbol{T}_{\boldsymbol{lk,p}}^{\boldsymbol{mrc}}$ and $\boldsymbol{T}_{\boldsymbol{lk,ip}}^{\boldsymbol{mrc}}$ calculated in the next lemma.

Lemma 1: The expected value of the effective channel matrices obtained by the MRC receiver, with perfect and imperfect CSI, i.e., $\boldsymbol{T}_{\boldsymbol{lk,p}}^{\boldsymbol{mrc}}$ and $\boldsymbol{T}_{\boldsymbol{lk,ip}}^{\boldsymbol{mrc}}$ are, respectively, calculated as follows:

$$E[\boldsymbol{T}_{\boldsymbol{lk,p}}^{\boldsymbol{mrc}}] = \sqrt{\beta_l \beta_k}\delta(l-k)\begin{pmatrix} E[g_0] & E[g_{-1}] & \cdots & E[g_{1-N}] \\ E[g_1] & E[g_0] & \cdots & E[g_{2-N}] \\ \vdots & \ddots & \ddots & \vdots \\ E[g_{N-1}] & E[g_{N-2}] & \cdots & E[g_0] \end{pmatrix} \tag{37}$$

$$\begin{aligned} E[\boldsymbol{T}_{\boldsymbol{lk,ip}}^{\boldsymbol{mrc}}] &= \sum_{j=1}^{K} \delta(j-k)\sqrt{\beta_j \beta_k} E[\lambda_{ljm}\boldsymbol{G}_{\boldsymbol{km}}] \\ &= \beta_k \begin{pmatrix} \gamma'_{lkk}(0) & \gamma'_{lkk}(-1) & \cdots & \gamma'_{lkk}(1-N) \\ \gamma'_{lkk}(1) & \gamma'_{lkk}(0) & \cdots & \gamma'_{lkk}(2-N) \\ \vdots & \ddots & \ddots & \vdots \\ \gamma'_{lkk}(N-1) & \gamma'_{lkk}(N-2) & \cdots & \gamma'_{lkk}(0) \end{pmatrix} \end{aligned} \tag{38}$$

Proof: The proof involves simple and straightforward calculations including the fact that $E[h_{lm}^{*}h_{km}] = \delta(l-k)$. ■

Eq. (37) shows that the expected value of the effective channel matrices from different users is zero except the one corresponding to the desired user. By using the law of large numbers,

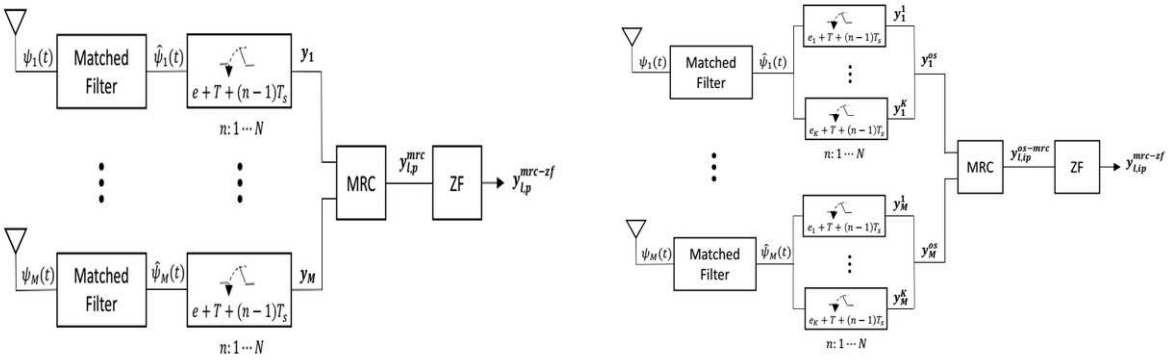

(a) MRC-ZF Receiver with perfect CSI

(b) MRC-ZF Receiver with imperfect CSI

Fig. 2: MRC-ZF Receiver

it can be shown that when M grows large, effective channel matrices approach their expected values. Therefore, IUI vanishes and the dominant degradation will be ISI caused by effective channel matrix of the desired user. On the other hand, Eq. (38) shows that the expected value of the effective channel matrices is nonzero for all users. It means that, even when M grows large, interference from other users still exist. Therefore, not only ISI but also IUI degrades the performance. We use the concept of zero forcing receiver to cancel the effect of these averaged matrices, however, other methods like minimum mean squared error (MMSE) and successive interference cancellation (SIC) can also be used. For perfect CSI scenario where only one nonzero effective channel matrix exists, the effect of the averaged ISI can be cancelled by multiplying the output sample of the MRC receiver by matrix $\boldsymbol{Z}$ which is defined as:

$$\boldsymbol{Z} = \begin{pmatrix} E[g_0] & E[g_{-1}] & \cdots & E[g_{1-N}] \\ E[g_1] & E[g_0] & \cdots & E[g_{2-N}] \\ \vdots & \ddots & \ddots & \vdots \\ E[g_{N-1}] & lE[g_{N-2}] & \cdots & E[g_0] \end{pmatrix}^{-1} \tag{39}$$

For the imperfect CSI scenario, because all the effective channel matrices are nonzero, we need extra set of equations to be able to cancel all interference terms. Therefore, we utilize the concept of oversampling as explained in [13], [12] and [14]. The receiver structure for the proposed methods are shown in Figures 2a and 2b. The description of these methods follows next.

1) MRC-ZF Receiver with Perfect CSI: As shown in Fig. 2a, the output samples of the MRC receiver are multiplied by $\boldsymbol{Z}$ to cancel the effect of the averaged ISI. Note that matrix $\boldsymbol{Z}$ is pre calculated once based on the pulse shape, sampling origin and delay distributions and then, it can be used during the entire transmission. We call this receiver MRC-ZF whose output samples are:

$$\boldsymbol{y_{l,p}^{mrc-zf}} = \sqrt{\rho_d} \sum_{k=1}^{K} \boldsymbol{T_{lk,p}^{mrc-zf}} \boldsymbol{b_k} + \boldsymbol{n_{l,p}^{mrc-zf}} \tag{40}$$

where $\boldsymbol{T_{lk,p}^{mrc-zf}} = \boldsymbol{Z}\boldsymbol{T_{lk,p}^{mrc}}$, $\boldsymbol{n_{l,p}^{mrc-zf}} = \boldsymbol{Z}\boldsymbol{n_{l,p}^{mrc}}$ and entries of matrix $\boldsymbol{T_{lk,p}^{mrc-zf}}$ are calculated as follows:

$$\boldsymbol{T_{lk,p}^{mrc-zf}}(n_1, n_2) = \frac{1}{M} \sum_{m=1}^{M} \sqrt{\beta_l \beta_k} h_{lm}^* h_{km} \sum_{i=1}^{N} Z(n_1, i) g(e + T + (i - n_2)T_s - \tau_{km}) \tag{41}$$

For the special case of symbol-level synchronization, i.e., $f(\tau) = \bar{\delta}(\tau)$, $\boldsymbol{Z}$ will be identity matrix; meaning that no additional processing is required which is in line with the works done in the literature. The expected value of matrix $\boldsymbol{T_{lk,p}^{mrc-zf}}$ is equal to $\delta(l-k)\boldsymbol{I_N}$ which means the effect of ISI diminishes for large values of M. The approximation of the achievable rate by the MRC-ZF receiver is presented in the next theorem.

Theorem 3: The achievable rate by each user using the MRC-ZF receiver can be approximated by:

$$R_{l,p}^{mrc-zf} \approx \log_2 \left(1 + \frac{\rho_d \beta_l (2\xi''_{a,a} + (M-1))}{\rho_d (\sum_{n=1}^{N} \xi''_{a,n}) \sum_{k=1}^{K} \beta_k + 2\rho_d \beta_l \sum_{\substack{n=1 \\ n \neq a}}^{N} \xi''_{a,n} + \epsilon_a} \right) \tag{42}$$

where $\xi''_{a,n} = E\left[\boldsymbol{G'}^2(a,n)\right]$ and $\epsilon_a = \boldsymbol{Z}\boldsymbol{Z}^H(a,a)$ are only functions of the distribution of delays and the pulse shape. Assuming the same distribution for all the time delays, receive antenna and user indices are discarded after taking expectations. Also note that due to the structure of the system, the achievable rate for different symbols of the frame except the I-boundary ones is the same, thus the index of a can be discarded.

Proof: The proof is presented in Appendix C. ■

By using the MRC-ZF receiver which exploits the statistics of unknown time delays, the effect of averaged ISI is vanished. If the number of receive antennas goes to infinity, the achievable rate goes to infinity. Therefore, we can scale down the transmit power and still provide the desirable

performance. In other words, if we choose $\rho_d = \frac{E_d}{M}$ in Eq. (42) and let M go to infinity, we will have:

$$R_{l,p}^{mrc-zf} \to \log_2\left(1 + \frac{E_d\beta_l}{\epsilon_a}\right), as\ M \to \infty, \rho_d = \frac{E_d}{M} \tag{43}$$

Hence, even in the presence of unknown time delays, the power scaling law is held by using the MRC-ZF receiver. The value of ϵ_a is calculated based on pulse shape, time delay distribution and sampling origin. The loss of ϵ_a is because of noise enhancement by ZF and can be mitigated by using other cancellation methods like MMSE and SIC which is topic of our future work.

2) MRC-ZF Receiver with Imperfect CSI: As explained before, when the channel coefficients are estimated by using orthogonal pilot sequences, the effective channel matrices for the K users are nonzero. Therefore, we need at least K sets of samples to be able to cancel them using ZF method. Denoting $\boldsymbol{y_m^t}, 1 \leq t \leq K$ as the set of N samples obtained at sampling times of $e_t + T + (n-1)T_s, n = 1, \cdots, N$, as shown in Fig. 2b, we can collect all samples obtained at receive antenna m in a vector $\boldsymbol{y_m^{os}} = [(\boldsymbol{y_m^1})^T, \cdots, (\boldsymbol{y_m^K})^T]^T$ to derive:

$$\boldsymbol{y_m^{os}} = \sqrt{\rho_d}\boldsymbol{T_m}\boldsymbol{b} + \boldsymbol{n_m^{os}} \tag{44}$$

where $\boldsymbol{b} = [\boldsymbol{b_1}^T, \cdots, \boldsymbol{b_K}^T]^T$ includes transmitted vectors of all users and $\boldsymbol{T_m}$ is defined as:

$$\boldsymbol{T_m} = \begin{pmatrix} \boldsymbol{T_{1m}^1} & \boldsymbol{T_{2m}^1} & \cdots & \boldsymbol{T_{Km}^1} \\ \boldsymbol{T_{1m}^2} & \boldsymbol{T_{2m}^2} & \cdots & \boldsymbol{T_{Km}^2} \\ \vdots & \ddots & \ddots & \vdots \\ \boldsymbol{T_{1m}^K} & \boldsymbol{T_{2m}^K} & \cdots & \boldsymbol{T_{Km}^K} \end{pmatrix} \tag{45}$$

where $\boldsymbol{T_{km}^t}$ represents the channel matrix of User k to receive antenna m in the tth set of samples, i.e., $\boldsymbol{T_{km}^t} = \sqrt{\beta_k}h_{km}\boldsymbol{G_{km}^t}$ where $\boldsymbol{G_{km}^t}$ is defined as Eq. (7) with $e = e_t$. The noise vector also includes all the noise vectors obtained from different sampling times, i.e., $\boldsymbol{n_m^{os}} = [(\boldsymbol{n_m^1})^T, \cdots, (\boldsymbol{n_m^K})^T]^T$ and its covariance matrix is calculated by:

$$\boldsymbol{\Sigma_{n^{os}}} = \begin{pmatrix} \boldsymbol{\Sigma_{11}} & \boldsymbol{\Sigma_{12}} & \cdots & \boldsymbol{\Sigma_{1K}} \\ \boldsymbol{\Sigma_{21}} & \boldsymbol{\Sigma_{22}} & \cdots & \boldsymbol{\Sigma_{2K}} \\ \vdots & \ddots & \ddots & \vdots \\ \boldsymbol{\Sigma_{K1}} & \boldsymbol{\Sigma_{K2}} & \cdots & \boldsymbol{\Sigma_{KK}} \end{pmatrix} \tag{46}$$

where $\boldsymbol{\Sigma_{t_1 t_2}}$ is the covariance matrix between noise samples obtained at times t_1 and t_2 defined as:

$$\boldsymbol{\Sigma_{t_1,t_2}} = \begin{pmatrix} g(T+(e_{t_1}-e_{t_2})) & \cdots & g(T+(1-N)T_s+(e_{t_1}-e_{t_2})) \\ g(T+T_s+(e_{t_1}-e_{t_2})) & \cdots & g(T+(2-N)T_s-(e_{t_1}-e_{t_2})) \\ \vdots & \ddots & \vdots \\ g(T+(N-1)T_s+(e_{t_1}-e_{t_2})) & \cdots & g(T+(e_{t_1}-e_{t_2}) \end{pmatrix} \tag{47}$$

The receive antenna index is discarded because the noise covariance matrix is the same at all receive antennas. The channel coefficient of User l to receive antenna m , i.e., $\tilde{c}^s_{lm}$ is equal to:

$$\tilde{c}^s_{lm} = \sum_{j=1}^{K} \lambda^s_{ljm} c_{jm} + \tilde{n}^s_{lm} \tag{48}$$

where λ_{ljm} is the "leakage factor" and is equal to:

$$\lambda^s_{ljm} = \sum_{i=-w}^{i=w} g(e_s + T + iT_s - \tau_{jm}) \boldsymbol{\Upsilon^i}(j,l) \tag{49}$$

After performing MRC for the lth user, the resulting system of equations is:

$$\boldsymbol{y^{os-mrc}_{l,ip}} = \sqrt{\rho_d} \boldsymbol{\hat{T}_l b} + \boldsymbol{n^{os-mrc}_{l,ip}} \tag{50}$$

where $\boldsymbol{\hat{T}_l}$ is the effective channel matrix:

$$\boldsymbol{\hat{T}_l} = \begin{pmatrix} \boldsymbol{\hat{T}^1_{l1}} & \boldsymbol{\hat{T}^1_{l2}} & \cdots & \boldsymbol{\hat{T}^1_{lK}} \\ \boldsymbol{\hat{T}^2_{l1}} & \boldsymbol{\hat{T}^2_{l2}} & \cdots & \boldsymbol{\hat{T}^2_{lK}} \\ \vdots & \ddots & \ddots & \vdots \\ \boldsymbol{\hat{T}^K_{l1}} & \boldsymbol{\hat{T}^K_{l2}} & \cdots & \boldsymbol{\hat{T}^K_{lK}} \end{pmatrix} \tag{51}$$

and each subblock, $\boldsymbol{\hat{T}^t_{lk}}$, is defined as:

$$\boldsymbol{\hat{T}^t_{lk}} = \frac{1}{M} \sum_{m=1}^{M} \left(\sum_{j=1}^{K} \lambda^s_{ljm} c^*_{jm} \right) \boldsymbol{T^t_{km}} \tag{52}$$

The effective noise is also calculated as:

$$\boldsymbol{n^{os-mrc}_{l,ip}} = \frac{\sqrt{\rho_d}}{M} \sum_{m=1}^{M} (\tilde{n}^s_{lm})^* \boldsymbol{T_m b} + \frac{1}{M} \sum_{m=1}^{M} \left(\sum_{j=1}^{K} \lambda^s_{ljm} c^*_{jm} + (\tilde{n}^s_{lm})^* \right) \boldsymbol{n^{os}_m} \tag{53}$$

Using Lemma 1, the expected value of $\hat{\boldsymbol{T}}_{\boldsymbol{l}}$ is equal to:

$$E[\hat{\boldsymbol{T}}_{\boldsymbol{l}}] = \begin{pmatrix} \boldsymbol{\Gamma}_{\boldsymbol{l1}}^{\boldsymbol{1}} & \boldsymbol{\Gamma}_{\boldsymbol{l2}}^{\boldsymbol{1}} & \cdots & \boldsymbol{\Gamma}_{\boldsymbol{lK}}^{\boldsymbol{1}} \\ \boldsymbol{\Gamma}_{\boldsymbol{l1}}^{\boldsymbol{2}} & \boldsymbol{\Gamma}_{\boldsymbol{l2}}^{\boldsymbol{2}} & \cdots & \boldsymbol{\Gamma}_{\boldsymbol{lK}}^{\boldsymbol{2}} \\ \vdots & \ddots & \ddots & \vdots \\ \boldsymbol{\Gamma}_{\boldsymbol{l1}}^{\boldsymbol{K}} & \boldsymbol{\Gamma}_{\boldsymbol{l2}}^{\boldsymbol{K}} & \cdots & \boldsymbol{\Gamma}_{\boldsymbol{lK}}^{\boldsymbol{K}} \end{pmatrix} \begin{pmatrix} \beta_1 \boldsymbol{I_N} & \boldsymbol{0} & \cdots & \boldsymbol{0} \\ \boldsymbol{0} & \beta_2 \boldsymbol{I_N} & \cdots & \boldsymbol{0} \\ \vdots & \ddots & \ddots & \vdots \\ \boldsymbol{0} & \boldsymbol{0} & \cdots & \beta_K \boldsymbol{I_N} \end{pmatrix}$$

$$= \boldsymbol{\Gamma_l} \begin{pmatrix} \beta_1 \boldsymbol{I_N} & \boldsymbol{0} & \cdots & \boldsymbol{0} \\ \boldsymbol{0} & \beta_2 \boldsymbol{I_N} & \cdots & \boldsymbol{0} \\ \vdots & \ddots & \ddots & \vdots \\ \boldsymbol{0} & \boldsymbol{0} & \cdots & \beta_K \boldsymbol{I_N} \end{pmatrix} \tag{54}$$

where $\boldsymbol{\Gamma}_{\boldsymbol{lk}}^{\boldsymbol{t}}$ is calculated as:

$$\boldsymbol{\Gamma}_{\boldsymbol{lk}}^{\boldsymbol{t}} = \begin{pmatrix} \gamma'_{lkkt}(0) & \gamma'_{lkkt}(-1) & \cdots & \gamma'_{lkkt}(1-N) \\ \gamma'_{lkkt}(1) & \gamma'_{lkkt}(0) & \cdots & \gamma'_{lkkt}(2-N) \\ \vdots & \ddots & \ddots & \vdots \\ \gamma'_{lkkt}(N-1) & \gamma'_{lkk}(N-2) & \cdots & \gamma'_{lkkt}(0) \end{pmatrix} \tag{55}$$

and its elements are equal to:

$$\begin{aligned} \gamma'_{lkkt}(i) &= E[\lambda^s_{lkm} g(e_t + T + iT_s - \tau_{km})] \\ &= \int_{-\infty}^{\infty} \left(\sum_{i=-w}^{i=w} \boldsymbol{\Upsilon^i}(k,l) g(e_s + T + iT_s - \tau_k) \right) g(e_t + T + iT_s - \tau_k) f(\tau_k) d\tau_k \end{aligned} \tag{56}$$

Matrix $\boldsymbol{\Gamma_l}$ in Eq. (54) is only related to sampling origins, e_ts, pilot sequences, pulse shape and delay distributions and it is known at the receiver. To resolve the problem of ISI and IUI, we calculate the inverse of $\boldsymbol{\Gamma_l}$ and denote it as $\boldsymbol{W_l}$, which is constructed by subblocks of $\boldsymbol{W_{lk}}$, i.e. $\boldsymbol{W_l} = [\boldsymbol{W_{l1}}^T, \cdots, \boldsymbol{W_{lK}}^T]^T$. Then, in order to detect the transmitted symbols of the lth user, we multiply the output of the MRC receiver, i.e. $\boldsymbol{y_l^{os-mrc}}$, by the lth subblock of $\boldsymbol{W_l}$, i.e. $\boldsymbol{W_{ll}}$. Therefore, the resulting samples will be:

$$\boldsymbol{y_{l,ip}^{mrc-zf}} = \sqrt{\rho_d} \sum_{k=1}^{K} \boldsymbol{T_{lk,ip}^{mrc-zf}} \boldsymbol{b_k} + \boldsymbol{n_{l,ip}^{mrc-zf}} \tag{57}$$

where $\boldsymbol{T_{lk,ip}^{mrc-zf}} = \boldsymbol{W_{ll}} \hat{\boldsymbol{T}}_{\boldsymbol{lk}}$, $\boldsymbol{n_{l,ip}^{mrc-zf}} = \boldsymbol{W_{ll}} \boldsymbol{n_{l,ip}^{os-mrc}}$ and $\hat{\boldsymbol{T}}_{\boldsymbol{lk}} = [(\boldsymbol{T_{lk}^1})^T, \ldots, (\boldsymbol{T_{lk}^K})^T]^T$. It is easy to show that, the expected value of matrix $\boldsymbol{T_{lk,ip}^{mrc-zf}}$ is equal to $\delta(l-k)\boldsymbol{I_N}$. Therefore, as M grows large, $\boldsymbol{T_{lk,ip}^{mrc-zf}}$ will be closer to its expected value and the effect of ISI and IUI converges to zero. The achievable rates for the aforementioned system is presented in the next theorem.

Theorem 4: The achievable rate by mapping the output samples of the MRC-ZF receiver using orthogonal channel estimation, when there is unknown time delays between received signals can be approximated by:

$$R_{l,ip}^{mrc-zf} \approx \log_2\left(1+\frac{desired\ signal}{IUI+ISI+noise}\right) \tag{58}$$

where desired signal, ISI, IUI and noise components are defined, respectively as:

$$desired\ signal = \rho_d\beta_l^2(2\hat{\gamma}''_{lll}(a,a)+(M-1))+\rho_d\beta_l\sum_{\substack{j=1\\j\neq l}}^{K}\beta_j\hat{\gamma}''_{ljl}(a,a)$$

$$ISI = \rho_d\beta_l^2\sum_{\substack{i=1\\i\neq a}}^{N}2\hat{\gamma}''_{lll}(a,i)+\rho_d\beta_l\sum_{\substack{j=1\\j\neq l}}^{K}\beta_j\sum_{\substack{i=1\\i\neq a}}^{N}\hat{\gamma}''_{ljl}(a,i)$$

$$IUI = \rho_d\sum_{\substack{k=1\\k\neq l}}^{K}\beta_k^2\sum_{i=1}^{N}2\hat{\gamma}''_{lkk}(a,i)+\rho_d\sum_{\substack{k=1\\k\neq l}}^{K}\sum_{\substack{j=1\\j\neq k}}^{K}\beta_k\beta_j\sum_{i=1}^{N}\hat{\gamma}''_{ljk}(a,i)$$

$$noise = \frac{\rho_d}{\rho_p}\boldsymbol{U_l}(a,a)\sum_{k=1}^{K}\beta_k+\left(\sum_{k=1}^{K}\beta_k\lambda''_{lk}+\frac{1}{\rho_p}\right)\boldsymbol{V_l}(a,a)$$

where $\boldsymbol{U_l}=\boldsymbol{W_{ll}}E[\hat{\boldsymbol{G}}_{\boldsymbol{km}}\hat{\boldsymbol{G}}_{\boldsymbol{km}}^H]\boldsymbol{W_{ll}^H}$ and $\boldsymbol{V_l}=\boldsymbol{W_{ll}}\boldsymbol{\Sigma_{n^{os}}}\boldsymbol{W_{ll}^H}$. Also,

$$\hat{\gamma}''_{ljk}(a,i)=\int_{-\infty}^{\infty}\int_{-\infty}^{\infty}\left(\lambda_{lj}^s\hat{\boldsymbol{G}}_{\boldsymbol{lkm}}(a,i)\right)^2 f(\tau_j)f(\tau_k)d\tau_j d\tau_k \tag{59}$$

$$E[\lambda''_{lk}]=\int_{-\infty}^{\infty}\left(\lambda_{lk}^s\right)^2 f(\tau_k)d\tau_k \tag{60}$$

where $\hat{\boldsymbol{G}}_{\boldsymbol{lkm}}(a,i)=\sum_{r=1}^{NK}\boldsymbol{W}_{ll}(a,r)\hat{\boldsymbol{G}}_{\boldsymbol{km}}(r,i)$ and $\hat{\boldsymbol{G}}_{\boldsymbol{km}}=[(\boldsymbol{G}_{\boldsymbol{km}}^{\boldsymbol{1}})^T,\cdots,(\boldsymbol{G}_{\boldsymbol{km}}^{\boldsymbol{K}})^T]^T$. Assuming the same distribution for all the time delays, receive antenna index is discarded after taking expectations. Again, note that due to the structure of the system, the achievable rate for different symbols of the frame except the I-boundary ones is the same, thus the index of a can be discarded.

Proof: The proof is presented in Appendix D. ■

By using the MRC-ZF receiver which exploits the statistics of unknown time delays, the effect of averaged ISI and IUI is vanished. If the number of receive antennas goes to infinity, the achievable rate goes to infinity. Replacing $\rho_d=\frac{E_d}{\sqrt{M}}$ in Eq. (58) and letting M go to infinity, we will have:

$$R_{l,ip}^{mrc-zf}\rightarrow\log_2\left(1+\frac{E_d\beta_l}{\boldsymbol{V_l}(a,a)}\right),as\ M\rightarrow\infty,\rho_d=\frac{E_d}{\sqrt{M}} \tag{61}$$

Hence, even in the presence of unknown time delays, the power scaling law is held by using the MRC-ZF receiver. The value of $\boldsymbol{V_l}(a,a)$ is calculated based on pulse shape, time delay distribution and sampling origin. Again, the loss of $\boldsymbol{V_l}(a,a)$ which is because of noise enhancement by ZF can be mitigated by using other cancellation methods like MMSE and SIC.

V. Simulation Results

In this section, simulation results are presented to verify our theoretical analysis. In the simulations, time delays follow the distribution mentioned in Eq. (3), noise samples and fading coefficients are also distributed as $CN(0,1)$. The large-scale channel fading is modelled as $\beta_k = z_k/(r_k/r_h)^v$, where z_k is a log-normal random variable with standard deviation of σ, v is the path-loss exponent, and r_k is the distance between the kth user and the BS which varies in the interval of $[r_h, R]$. We have assumed that $v = 1.8$, $\sigma = 8$, $r_h = 100$ and $R = 1000$. In Fig. 3, the performance of the MRC receiver with perfect CSI is presented by theoretical approximation in Theorem 1 and via simulation. The sum rate for 5 users are plotted with respect to the number of receive antennas. The results include rectangular (Rect.) pulse shape and raised cosine (R.C.) pulse shape with roll-off factor of $\beta = 0.5$. Different sampling origins (e) are used to show the effect of e in the performance. Our theoretical approximation and simulation results match. It also shows that, unknown time delays limit the performance, and by increasing M, the sum rate is saturated. Although changing the sampling origin does not eliminate the performance limit, it can provide about 10 bpcu gain in the sum rate which is around 100% increase in the achievable rate. Fig. 4 shows the asymptotic performance, i.e. $M \to \infty$, with respect to the sampling origin. It includes the result for different number of users, $K = [2, 5, 15]$, and as the number of users increases, the optimal value of e tends to half which verifies the results in table I. This is in line with the fact that for small number of users the distribution in Eq. (3) is closer to a delta function whose optimal sampling origin is $e = 0$. By increasing the number of users, the distribution tends to uniform whose best sampling origin is half. In Fig. 5, the performance of the MRC-ZF receiver with perfect CSI is presented. By increasing M, the sum rate increases without bound unlike the MRC receiver whose sum rate is limited. Different values of e are included to show the effect of sampling origin. Around 5 bpcu additional rate can be achieved by appropriate choice of e. In Fig. 6, the sum rate for the MRC receiver with imperfect CSI is presented. It shows that the sum rate is limited due to ISI and IUI and increasing M does not change the sum rate much. However, changing the sampling origin can slightly improve the performance.

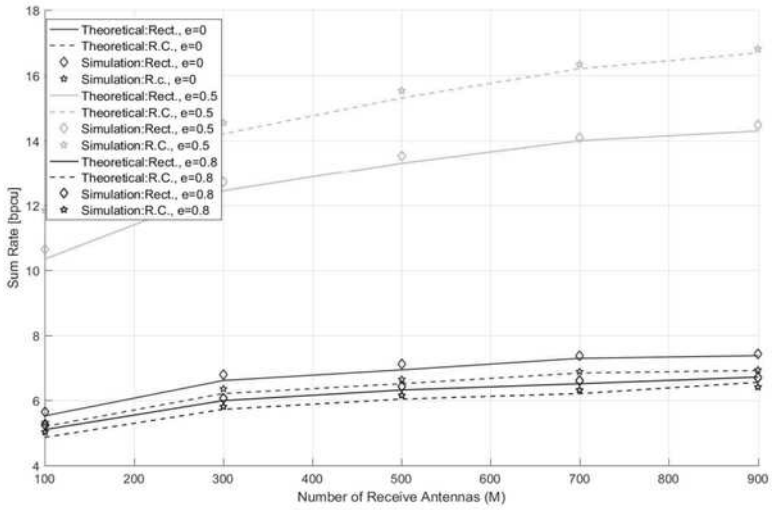

Fig. 3: Performance of the MRC receiver with respect to number of receive antennas, using perfect CSI for 5 users each of them using 20 dB transmit power and different number of receive antennas

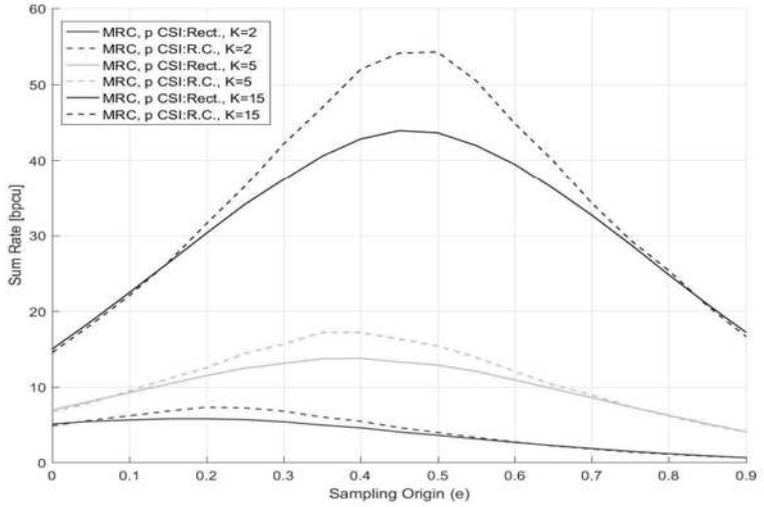

Fig. 4: Asymptotic performance of the MRC receiver with respect to sampling origin for different number of users, using perfect CSI and $\rho_d = 20$ dB

In Fig. 7, the asymptotic performance of the MRC receiver with respect to sampling origin is presented. Again, we observe that, by increasing the number of users, the optimal sampling origin tends to half. In Fig. 8, the performance of the MRC-ZF receiver with imperfect CSI is presented. Number of users is equal to 5 and 5 sets of samples are obtained by sampling at

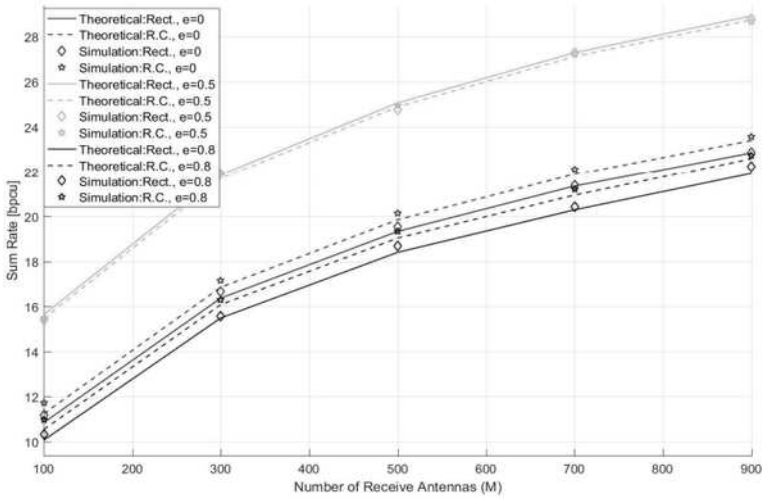

Fig. 5: Performance of the MRC-ZF receiver with different sampling origins, using perfect CSI for 5 users each of them using 20 dB transmit power and different number of receive antennas

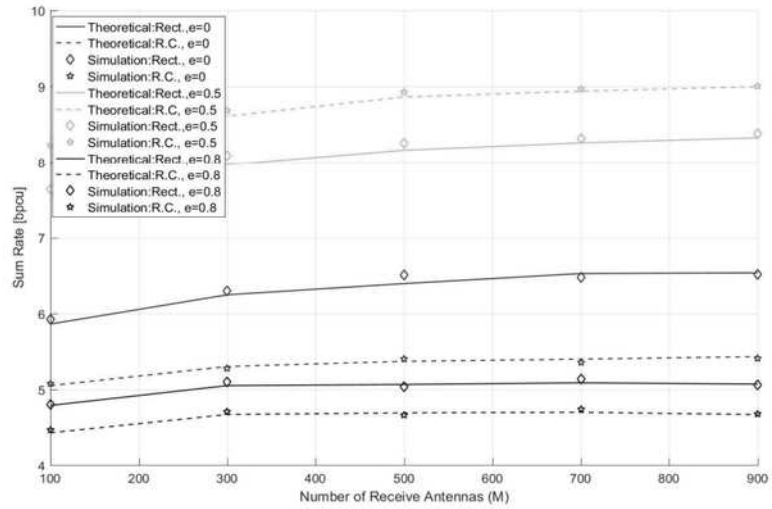

Fig. 6: Performance of the MRC receiver with different sampling origins, using imperfect CSI for 5 users each of them using 20 dB transmit power and different number of receive antennas

times uniformly distributed between $(0, 1)$, i.e, $e_t = \frac{t}{6}, 1 \leq t \leq 5$. It shows that, by increasing M, the sum rate achieved by the MRC-ZF receiver can be increased without saturation. The simulation results and theoretical approximation in Theorem 4 are also very close which verifies the analysis. In Fig. 9, the performance of the MRC and the MRC-ZF receivers are presented while $\rho_d = \frac{E_d}{M}$ and M is very large. Increasing E_d does not increase the sum rate achieved by

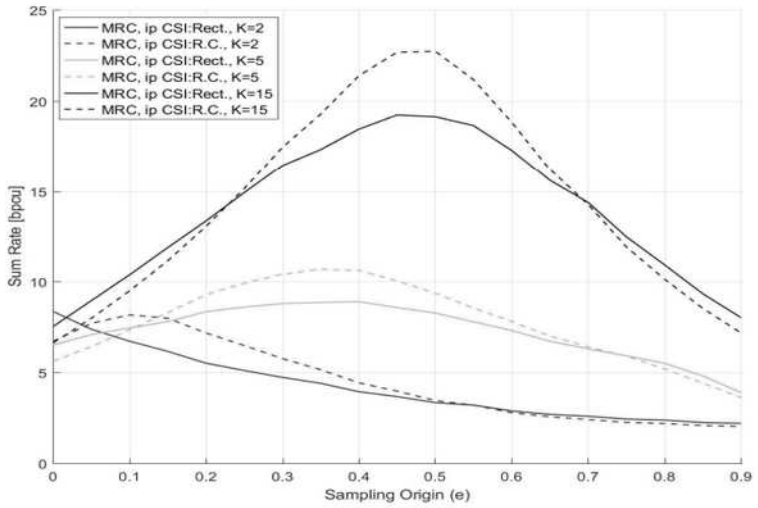

Fig. 7: Performance of the MRC receiver for different number of users with respect to sampling origin, using imperfect CSI. Each users uses 20 dB transmit power and the number of receive antennas goes to infinity

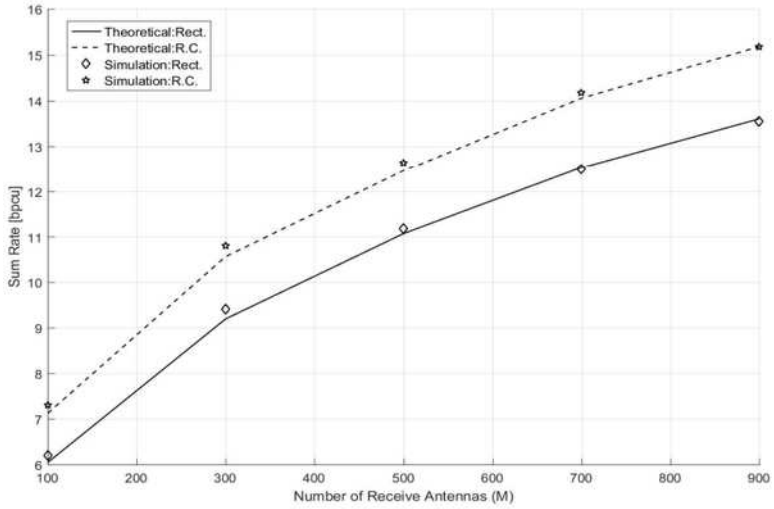

Fig. 8: Performance of the MRC-ZF receiver with uniform oversampling, using imperfect CSI for 5 users each of them using 20 dB transmit power and different number of receive antennas

the MRC receiver whereas, in the MRC-ZF receiver the achievable sum rate increases by E_d showing that by using the MRC-ZF the scaling power law can be achieved. In Fig. 10, a similar analysis is presented for imperfect CSI with a power scale of $\frac{1}{\sqrt{M}}$. Again, it verifies our claim that the MRC receiver is unable to hold the power scale law when there is time delay between

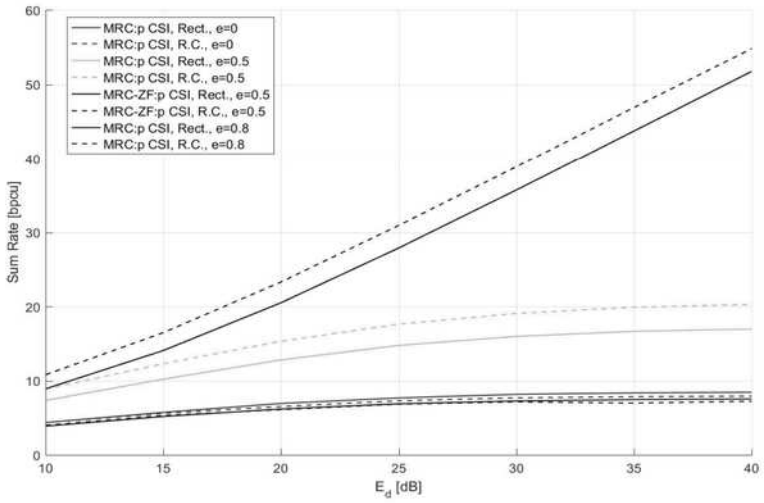

Fig. 9: Comparison of the MRC receiver with different sampling origins and the MRC-ZF receiver, using perfect CSI for 5 users when M goes to infinity and $\rho_d = \frac{E_d}{M}$

received signals. However, by implementing the MRC-ZF, a power scale of $\frac{1}{\sqrt{M}}$ is achieved.

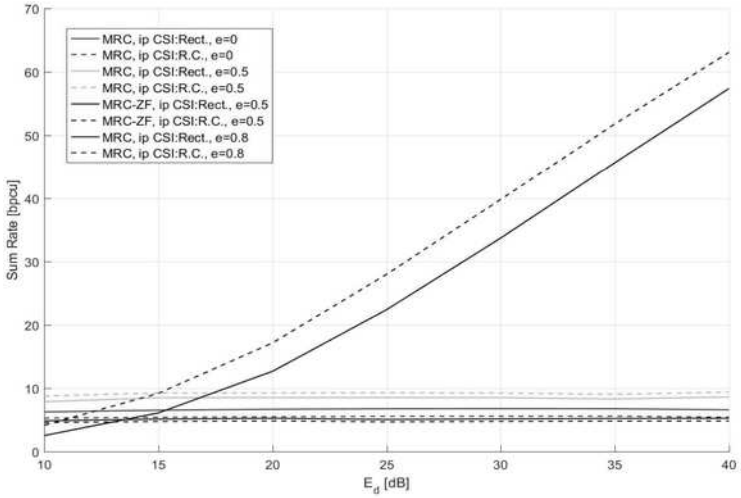

Fig. 10: Comparison of the MRC receiver with different sampling origins and the MRC-ZF receiver, using imperfect CSI for 5 users when M goes to infinity and $\rho_d = \frac{E_d}{\sqrt{M}}$

VI. Conclusion

In this work, we obtained the general formula for the achievable rate by the MRC receiver when unknown timing mismatch exists. We showed that unknown timing mismatch degrades

the performance substantially. In other words, in the presence of unknown timing mismatch, the achievable rate by each user is limited when the number of receive antennas goes to infinity. To address this challenge, we introduced two receiver design methods, one when the perfect CSI is available and one when CSI is estimated by orthogonal pilot sequences, which restore the benefits of massive MIMO. We proved that these introduced receivers follow the power scale law, i.e., single user performance can be achieved by using arbitrary small transmit power. In our proposed receiver designs, we used ZF method to cancel the effect of averaged ISI and IUI, however, other methods like MMSE or SIC can also be used. We also used oversampling besides ZF to cancel the effect of contamination in the channel estimations caused by timing mismatch. This method can be adopted to address the similar problem of "pilot contamination" which is topic of our future work. At the end, we presented simulation results which confirmed our analysis.

APPENDIX A

We analyzed four different receiver structures, including: MRC with perfect and imperfect CSI and MRC-ZF with perfect and imperfect CSI. The output sample of either of these receivers for detection of the ath symbol of the lth user can be written in a general framework as:

$$\boldsymbol{y}_{\boldsymbol{l,p/ip}}^{\boldsymbol{mrc/mrc-zf}}(a) = \sqrt{\rho_d}\sum_{k=1}^{K}\sum_{n=1}^{N}\boldsymbol{T}_{\boldsymbol{lk,p/ip}}^{\boldsymbol{mrc/mrc-zf}}(a,n)\boldsymbol{b_k}(n) + \boldsymbol{n}_{\boldsymbol{l,p/ip}}^{\boldsymbol{mrc/mrc-zf}}(a) \tag{62}$$

Discarding the subscripts for different receivers, the corresponding achievable rate can be calculated as follows [17]:

$$R_l(a) = E\left[\log_2\left(1+\frac{\rho_d|\boldsymbol{T_{ll}}(a,a)|^2}{\rho_d\sum_{\substack{k=1\\k\neq l}}^{K}\sum_{n=1}^{N}|\boldsymbol{T_{lk}}(a,n)|^2+\rho_d\sum_{\substack{n=1\\n\neq a}}^{N}|\boldsymbol{T_{ll}}(a,n)|^2+|\boldsymbol{n_l}(a)|^2}\right)\right] \tag{63}$$

To approximate the above expression, we use the following lemma:

Lemma 2: Given any two positive random variables, X and Y, we have the following identity:

$$\left|E\left[\log_2\left(1+\frac{X}{Y}\right)\right]-\log_2\left(1+\frac{E[X]}{E[Y]}\right)\right| \leq \log_2\left(E[X+Y]E\left[\frac{1}{X+Y}\right]E[Y]E\left[\frac{1}{Y}\right]\right) \tag{64}$$

Proof: We know that $f(x) = \log_2(x)$ and $g(x) = \log_2(\frac{1}{x})$ are concave and convex functions, respectively. Hence, by using Jensen's inequality, we can get the following bounds:

$$\log_2\left(\frac{1}{E\left[\frac{1}{Y}\right]}\right) \leq E\left[\log_2(Y)\right] \leq \log_2\left(E[Y]\right) \tag{65}$$

$$\log_2\left(\frac{1}{E\left[\frac{1}{X+Y}\right]}\right) \leq E\left[\log_2\left(X+Y\right)\right] \leq \log_2\left(E[X+Y]\right) \tag{66}$$

By combining these inequalities, we can conclude that:

$$\log_2\left(\frac{1}{E\left[\frac{1}{X+Y}\right]}\right) - \log_2\left(E[Y]\right) \leq E\left[\log_2(X+Y)\right] - E\left[\log_2(Y)\right] \leq \log_2(E[X+Y]) - \log_2\left(\frac{1}{E\left[\frac{1}{Y}\right]}\right) \tag{67}$$

$$\log_2\left(\frac{1}{E\left[\frac{1}{X+Y}\right]}\right) - \log_2(E[Y]) \leq \log_2(E[X+Y]) - \log_2(E[Y]) \leq \log_2(E[X+Y]) - \log_2\left(\frac{1}{E\left[\frac{1}{Y}\right]}\right) \tag{68}$$

We know that if $A \leq x \leq B$ and $A \leq y \leq B$, then $|x-y| \leq B-A$. Therefore, $\left|E\left[\log_2\left(1+\frac{X}{Y}\right)\right] - \log_2\left(1+\frac{E[X]}{E[Y]}\right)\right|$ is upper-bounded by $\log_2\left(E[X+Y]\right) - \log_2\left(\frac{1}{E\left[\frac{1}{Y}\right]}\right) - \log_2\left(\frac{1}{E\left[\frac{1}{X+Y}\right]}\right) + \log_2\left(E[Y]\right)$. After some calculations, the upper-bound can be simplified to $\log_2\left(E[X+Y]E\left[\frac{1}{X+Y}\right]E[Y]E\left[\frac{1}{Y}\right]\right)$ which completes the proof. ■

By applying a Taylor series expansion of $\frac{1}{Y}$ around $E[Y]$, we will have:

$$E\left[\frac{1}{Y}\right] = \frac{1}{E[Y]} + O\left(\frac{VAR[Y]}{E^3[Y]}\right) \tag{69}$$

as $\frac{VAR[Y]}{E[Y]} \to 0$ [24]. Eq. (69), implies that there exist positive numbers ϵ and C such that:

$$E\left[\frac{1}{Y}\right] \leq \frac{1}{E[Y]} + C\frac{VAR[Y]}{E^3[Y]} \quad when\ \frac{VAR[Y]}{E[Y]} \leq \epsilon \tag{70}$$

In Eq. (63), $\boldsymbol{T_{lk}}(a,n)$ is equal to the average of M independent R.V.s, i.e., $\boldsymbol{T_{lk}}(a,n) = \frac{1}{M}\sum_{i=1}^{M} t_{lk}^{i}(a,n)$. The expected value and variance of each summand is denoted as $\mu_{lk}(a,n)$ and $\sigma_{lk}^2(a,n)$, respectively. As a result, the expected value and variance of $\boldsymbol{T_{lk}}(a,n)$ are equal to $\mu_{lk}(a,n)$ and $\frac{1}{M}\sigma_{lk}^2(a,n)$, respectively. Then, $E[|\boldsymbol{T_{lk}}(a,n)|^2]$ and $VAR[|\boldsymbol{T_{lk}}(a,n)|^2]$ can be bounded by:

$$VAR[|\boldsymbol{T_{lk}}(a,n)|^2] \leq \frac{4}{M}\mu_{lk}^2(a,n)\sigma_{lk}^2(a,n) \tag{71}$$

$$E[|\boldsymbol{T_{lk}}(a,n)|^2] \geq \mu_{lk}^2(a,n) \tag{72}$$

where Inequality (72) is a result of Jensen's inequality and Inequality (71) is derived using Taylor approximation, i.e., $VAR[f(X)] = (f'(E[X]))^2 VAR[X] - \frac{(f''(E[X]))^2}{4} VAR^2[X]$. After some calculations, it can be shown that $\frac{VAR[Y]}{E^2[Y]}$ and $\frac{VAR[X+Y]}{E^2[X+Y]}$ can be made sufficiently small by increasing M, i.e, the number of receiver antennas, and as a result we have:

$$\left| E\left[\log_2\left(1+\frac{X}{Y}\right)\right] - \log_2\left(1+\frac{E[X]}{E[Y]}\right)\right| \leq \log_2\left(\left(1+C_1\frac{VAR[X+Y]}{E^2[X+Y]}\right)\left(1+C_2\frac{VAR[Y]}{E^2[Y]}\right)\right) \tag{73}$$

Finally, by using the bounds in (71) and (72), we can conclude that:

$$|R_l(a) - \tilde{R}_l(a)| \leq 2\log_2\left(1+\frac{c\sigma^2}{M\mu^2}\right) \tag{74}$$

where $\tilde{R}_l(a)$ is equal to:

$$\tilde{R}_l(a) = \log_2\left(1+\frac{\rho_d E[|\boldsymbol{T_{ll}}(a,a)|^2]}{\rho_d \sum_{\substack{k=1\\k\neq l}}^{K}\sum_{n=1}^{N} E[|\boldsymbol{T_{lk}}(a,n)|^2] + \rho_d \sum_{\substack{n=1\\n\neq a}}^{N} E[|\boldsymbol{T_{ll}}(a,n)|^2] + VAR[\boldsymbol{n_l}(a)]}\right) \tag{75}$$

$\mu = \min_{l,k,n} \mu_{lk}^2(a,n)$, $\sigma^2 = \max_{l,k,n} 4\mu_{lk}^2(a,n)\sigma_{lk}^2(a,n)$ and c is a constant. Inequality (74) shows that for sufficiently large values of M, the achievable rate can be approximated by $\tilde{R}_l(a)$ presented in Eq. (75). When M grows large, the approximation becomes tighter and $\tilde{R}_l(a) \to R_l(a)$ as M goes to infinity which is line with the fact that variables get close to determinitic values as M grows large. Simulation results also show that for M larger than 100, the approximation is very precise. Hence, for finding the achievable rates for different receivers, we just need to calculate the values of $E[|\boldsymbol{T_{lk}}(a,n)|^2]$ and the variance of effective noise vector for different receivers. For the MRC receiver with perfect CSI, $\boldsymbol{T_{lk,p}^{mrc}} = \frac{1}{M}\sum_{m=1}^{M}\sqrt{\beta_l\beta_k}h_{lm}^* h_{km}\boldsymbol{G_{km}}$ and the values of $E[|\boldsymbol{T_{lk}}(a,n)|^2]$ are calculated in the next lemma.

Lemma 3: The expected value of $|\boldsymbol{T_{lk,p}^{mrc}}(a,n)|^2$ can be calculated as follows:

$$E\left[|\boldsymbol{T_{lk,p}^{mrc}}(a,n)|^2\right] = \begin{cases} \frac{\beta_l^2}{M^2}\left(2ME[g_{n-a}^2] + M(M-1)E[g_{n-a}]^2\right) & k=l \\ \frac{\beta_l\beta_k}{M^2}(ME[g_{n-a}^2]) & k\neq l \end{cases} \tag{76}$$

Proof:

Case $k = l$:

$$E\left[|\boldsymbol{T}^{\boldsymbol{mrc}}_{\boldsymbol{ll,p}}(a,n)|^2\right] = \frac{1}{M^2}E\left[\left(\sum_{m=1}^{M}\beta_l|h_{lm}|^2\boldsymbol{G_{lm}}(a,n)\right)\left(\sum_{m=1}^{M}\beta_l|h_{lm}|^2\boldsymbol{G_{lm}}(a,n)\right)\right]$$

$$= \frac{\beta_l^2}{M^2}\left(\sum_{m=1}^{M}E\left[|h_{lm}|^4\boldsymbol{G^2_{lm}}(a,n)\right] + \sum_{m_1=1}^{M}\sum_{\substack{m_2=1\\m_2\neq m_1}}^{M}E\left[|h_{lm_1}|^2\boldsymbol{G_{km_1}}(a,n)|h_{lm_2}|^2\boldsymbol{G_{lm_2}}(a,n)\right]\right)$$

$$= \frac{\beta_l^2}{M^2}\left(2\sum_{m=1}^{M}E\left[\boldsymbol{G^2_{lm}}(a,n)\right] + \sum_{m_1=1}^{M}\sum_{\substack{m_2=1\\m_2\neq m_1}}^{M}E\left[\boldsymbol{G_{lm_1}}(a,n)\right]E\left[\boldsymbol{G_{lm_2}}(a,n)\right]\right)$$

$$= \frac{\beta_l^2}{M^2}\left(2ME\left[\boldsymbol{G}^2(a,n)\right] + M(M-1)E^2\left[\boldsymbol{G}(a,n)\right]\right) \tag{77}$$

where $\boldsymbol{G}$ is defined similar to $\boldsymbol{G_{km}}$, except that the indices of receive antenna and user are dropped because all the delays are assumed to have the same distribution from different users at different receive antennas. Denoting $E\left[\boldsymbol{G}(a,n)\right]$ as $E[g_{a-n}]$ which is defined below, completes the proof for the case $k = l$.

$$E[g_i] = \int_{-\infty}^{\infty} g(e+T+iT_s-\tau)f(\tau)d\tau \tag{78}$$

Note that $E[g_i]$ is nonzero only for $-I \leq i \leq I$.

Case $k \neq l$:

$$E\left[|\boldsymbol{T}^{\boldsymbol{mrc}}_{\boldsymbol{lk,p}}(a,n)|^2\right] = \frac{1}{M^2}E\left[\left(\sum_{m=1}^{M}\sqrt{\beta_l\beta_k}h^*_{lm}h_{km}\boldsymbol{G_{km}}(a,n)\right)\left(\sum_{m=1}^{M}\sqrt{\beta_l\beta_k}h_{lm}h^*_{km}\boldsymbol{G_{km}}(a,n)\right)\right]$$

$$= \frac{\beta_l\beta_k}{M^2}\left(\sum_{m=1}^{M}E\left[|h_{lm}|^2|h_{km}|^2\boldsymbol{G^2_{km}}(a,n)\right]\right)$$

$$= \frac{\beta_l\beta_k}{M^2}\left(\sum_{m=1}^{M}E\left[\boldsymbol{G^2_{km}}(a,n)\right]\right)$$

$$= \frac{\beta_l\beta_k}{M^2}\left(ME\left[\boldsymbol{G}^2(a,n)\right]\right)$$

$$= \frac{\beta_l\beta_k}{M^2}(ME[g^2_{n-a}]) \tag{79}$$

■

Covariance matrix of the effective noise vector is also calculated as:

$$\begin{aligned} COV[\boldsymbol{n}_{\boldsymbol{l,p}}^{\boldsymbol{mrc}}(a)] &= E\left[\boldsymbol{n}_{\boldsymbol{l,p}}^{\boldsymbol{mrc}}\boldsymbol{n}_{\boldsymbol{l,p}}^{\boldsymbol{mrc}H}\right] \\ &= E\left[\left(\frac{\sqrt{\beta_l}}{M}\sum_{m=1}^{M}h_{lm}^{*}\boldsymbol{n_m}\right)\left(\frac{\sqrt{\beta_l}}{M}\sum_{m=1}^{M}h_{lm}\boldsymbol{n_m^H}\right)\right] \\ &= \frac{\beta_l}{M^2}\sum_{m=1}^{M}E\left[|h_{lm}^2|\right]E\left[\boldsymbol{n_m}\boldsymbol{n_m^H}\right] \\ &= \frac{\beta_l}{M}\boldsymbol{I_N} \end{aligned} \tag{80}$$

By inserting the expected values of $|\boldsymbol{T}_{\boldsymbol{lk,p}}^{\boldsymbol{mrc}}(a,n)|^2$ and also the variance of the effective noise vector, we have:

$$\tilde{R}_{l,p}^{mrc} \approx \log_2\left(1+\frac{\rho_d\beta_l(2E[g_0^2]+(M-1)E[g_0]^2)}{\rho_d\sum\limits_{i=-I}^{I}E[g_i^2]\sum_{k=1}^{K}\beta_k+\rho_d\beta_l\sum\limits_{\substack{i=-I\\i\neq 0}}^{I}(2E[g_i^2]+(M-1)E[g_i]^2)+1}\right) \tag{81}$$

which completes the proof.

APPENDIX B

In the MRC receiver using the estimated CSI, the effective channel matrices denoted by $\boldsymbol{T}_{\boldsymbol{lk,ip}}^{\boldsymbol{mrc}}$ are equal to $\frac{1}{M}\sum_{m=1}^{M}\sum_{j=1}^{K}\lambda_{ljm}\sqrt{\beta_j\beta_k}h_{jm}^{*}h_{km}\boldsymbol{G_{km}}$. The value of λ_{ljm} is the leakage factor of unwanted users for the estimation of the desired channel and is equal to $\sum_{i=-w}^{i=w}g(e+T+iT_s-\tau_{jm})\boldsymbol{\Upsilon^i}(j,l)$.

Lemma 4: The expected value of $|\boldsymbol{T}_{\boldsymbol{lk,ip}}^{\boldsymbol{mrc}}(a,n)|^2$ is:

$$\begin{aligned} &E\left[|\boldsymbol{T}_{\boldsymbol{lk,ip}}^{\boldsymbol{mrc}}(a,n)|^2\right] = \\ &= \frac{1}{M^2}\left\{\beta_k^2\left(2M\gamma_{lkk}''(n-a)+M(M-1)(\gamma_{lkk}'(n-a))^2\right)+\sum_{\substack{j=1\\j\neq k}}^{K}\beta_j\beta_k(M\gamma_{ljk}''(n-a))\right\} \end{aligned} \tag{82}$$

where $\gamma_{ljk}''(n-a)=E[\gamma_{ljkm}^2(n-a)]$ and $\gamma_{ljk}'(n-a)=E[\gamma_{ljkm}(n-a)]$ are the expectations over the distributions. Note that, the receive antenna index is discarded after taking expectations. Also, $\gamma_{ljk}''(n-a)$ and $\gamma_{ljk}''(n-a)$ are nonzero only when $-I\leq n-a\leq I$.

Proof:

$$E\left[|\boldsymbol{T}^{\boldsymbol{mrc}}_{\boldsymbol{lk,ip}}(a,n)|^2\right] =$$
$$= \frac{1}{M^2}E\left[\left(\sum_{m=1}^{M}\sum_{j=1}^{K}\lambda_{ljm}\sqrt{\beta_j\beta_l}h^*_{jm}h_{km}\boldsymbol{G}_{\boldsymbol{km}}(a,n)\right)\left(\sum_{m=1}^{M}\sum_{j=1}^{K}\lambda_{ljm}\sqrt{\beta_j\beta_l}h_{jm}h^*_{km}\boldsymbol{G}_{\boldsymbol{km}}(a,n)\right)\right]$$
$$= \frac{1}{M^2}E\left[\sum_{j=1}^{K}\left(\sum_{m=1}^{M}\lambda_{ljm}\sqrt{\beta_j\beta_l}h^*_{jm}h_{km}\boldsymbol{G}_{\boldsymbol{km}}(a,n)\right)\sum_{j=1}^{K}\left(\sum_{m=1}^{M}\lambda_{ljm}\sqrt{\beta_j\beta_l}h_{jm}h^*_{km}\boldsymbol{G}_{\boldsymbol{km}}(a,n)\right)\right] \tag{83}$$

Due to independence between channel coefficients with different index, we have:

$$E\left[|\boldsymbol{T}^{\boldsymbol{mrc}}_{\boldsymbol{lk,ip}}(a,n)|^2\right] = \frac{1}{M^2}\left\{E\left[\left(\sum_{m=1}^{M}\beta_k|h_{km}|^2\gamma_{lkkm}(n-a)\right)\left(\sum_{m=1}^{M}\beta_k|h_{km}|^2\gamma_{lkkm}(n-a)\right)\right]\right.$$
$$\left.+\sum_{\substack{j=1\\j\neq k}}^{K}E\left[\left(\sum_{m=1}^{M}\sqrt{\beta_j\beta_k}h^*_{jm}h_{km}\gamma_{ljkm}(n-a)\right)\left(\sum_{m=1}^{M}\sqrt{\beta_j\beta_k}h_{jm}h^*_{km}\gamma_{ljkm}(n-a)\right)\right]\right\} \tag{84}$$

where $\gamma_{ljkm}(n-a) = \lambda_{ljm}\boldsymbol{G}_{\boldsymbol{km}}(a,n)$. Using the results in Lemma 3, we have:

$$E\left[|\boldsymbol{T}^{\boldsymbol{mrc}}_{\boldsymbol{lk,ip}}(a,n)|^2\right] =$$
$$\frac{1}{M^2}\left\{\beta_k^2\left(2M\gamma''_{lkk}(n-a)+M(M-1)(\gamma'_{lkk}(n-a))^2\right)+\sum_{\substack{j=1\\j\neq k}}^{K}\beta_j\beta_k(M\gamma''_{ljk}(n-a))\right\} \tag{85}$$

■

The effective noise vector is equal to:

$$\boldsymbol{n}^{\boldsymbol{mrc}}_{\boldsymbol{l,ip}} = \frac{\sqrt{\rho_d}}{M}\sum_{m=1}^{M}\tilde{n}_{lm}\sum_{k=1}^{K}\sqrt{\beta_k}h_{km}\boldsymbol{G}_{\boldsymbol{km}}\boldsymbol{b}_{\boldsymbol{k}}+\frac{1}{M}\sum_{m=1}^{M}\left(\sum_{j=1}^{K}\lambda_{ljm}\sqrt{\beta_j}h^*_{jm}+\tilde{n}_{lm}\right)\boldsymbol{n}_{\boldsymbol{m}} \tag{86}$$

where $\tilde{n}_{lm}$ is the estimation noise which is Gaussian and its variance is $\frac{1}{\rho_p}$. After some calculations, it can be shown that the variance of the ath element of the noise vector is equal to:

$$VAR[\boldsymbol{n}^{\boldsymbol{mrc}}_{\boldsymbol{l,ip}}(a)] = \frac{\rho_d}{M\rho_p}\sum_{k=1}^{K}\beta_k\sum_{i=-w}^{w}E[g_i^2]+\frac{1}{M}\left(\sum_{j=1}^{K}\beta_j\lambda''_{lj}+\frac{1}{\rho_p}\right) \tag{87}$$

where $\lambda''_{lj} = E[\lambda^2_{ljm}]$ is the average of λ^2_{ljm} over the delay distributions. Finally, by inserting the expected values of $|\boldsymbol{T}^{\boldsymbol{mrc}}_{\boldsymbol{lk,ip}}(a,n)|^2$ and also the variance of noise samples into Eq. (74), we achieve the following result:

$$\tilde{R}^{mrc}_{l,ip} \approx \log_2\left(1+\frac{desired\ signal}{IUI+ISI+noise}\right) \tag{88}$$

where the desired signal, ISI, IUI and noise components are defined as follows, respectively:

$$desired\ signal = \rho_d\beta_l^2(2\gamma''_{lll}(0)+(M-1)(\gamma'_{lll}(0))^2)) + \rho_d\beta_l\sum_{\substack{j=1\\j\neq l}}^{K}\beta_j\gamma''_{ljl}(0)$$

$$ISI = \rho_d\beta_l^2\sum_{\substack{i=-I\\i\neq 0}}^{I}(2\gamma''_{lll}(i)+(M-1)(\gamma'_{lll}(i))^2) + \rho_d\beta_l\sum_{\substack{j=1\\j\neq l}}^{K}\beta_j\sum_{\substack{i=-I\\i\neq 0}}^{I}\gamma''_{ljl}(i)$$

$$IUI = \rho_d\sum_{\substack{k=1\\k\neq l}}^{K}\beta_k^2\sum_{i=-I}^{I}(2\gamma''_{lkk}(i)+(M-1)(\gamma'_{lkk}(i))^2) + \rho_d\sum_{\substack{k=1\\k\neq l}}^{K}\sum_{\substack{j=1\\j\neq k}}^{K}\beta_k\beta_j\sum_{i=-I}^{I}\gamma''_{ljk}(i)$$

$$noise = \frac{\rho_d}{\rho_p}\sum_{k=1}^{K}\beta_k\sum_{i=-I}^{I}E[g_i^2] + \sum_{k=1}^{K}\beta_k\lambda''_{lk} + \frac{1}{\rho_p}$$

which completes the proof.

APPENDIX C

In MRC-ZF receiver with perfect CSI, $\boldsymbol{T}^{\boldsymbol{mrc-zf}}_{\boldsymbol{lk,p}} = \boldsymbol{Z}\boldsymbol{T}^{\boldsymbol{mrc}}_{\boldsymbol{lk,p}}$ and matrix $\boldsymbol{Z}$ is defined by Eq. (39). $\boldsymbol{n}^{\boldsymbol{mrc-zf}}_{\boldsymbol{l,p}}$ is also defined as $\boldsymbol{Z}\boldsymbol{n}^{\boldsymbol{mrc}}_{\boldsymbol{l,p}}$.

Lemma 5: The expected value of $|\boldsymbol{T}^{\boldsymbol{mrc-zf}}_{\boldsymbol{lk,p}}(a,n)|^2$ can be calculated as follows:

$$E\left[|\boldsymbol{T}^{\boldsymbol{mrc-zf}}_{\boldsymbol{lk,p}}(a,n)|^2\right] = \begin{cases} \frac{\beta_l^2}{M^2}(2M\xi^2_{a,n}+M(M-1)\delta(a-n)) & k=l \\ \frac{\beta_l\beta_k}{M^2}(M\xi^2_{a,n}) & k\neq l \end{cases} \tag{89}$$

Proof: Case $k = l$:

$$
\begin{aligned}
E\left[|\boldsymbol{T}^{\boldsymbol{mrc}}_{\boldsymbol{ll,p}}(a,n)|^2\right] &= \frac{1}{M^2} E\left[\left(\sum_{m=1}^{M} \beta_l |h_{lm}|^2 \boldsymbol{G'_{lm}}(a,n)\right)\left(\sum_{m=1}^{M} \beta_l |h_{lm}|^2 \boldsymbol{G'_{lm}}(a,n)\right)\right] \\
&= \frac{\beta_l^2}{M^2}\left(\sum_{m=1}^{M} E\left[|h_{lm}|^4 \boldsymbol{G'^2_{lm}}(a,n)\right] + \right. \\
&\qquad \left. \sum_{m_1=1}^{M}\sum_{\substack{m_2=1 \\ m_2\neq m_1}}^{M} E\left[|h_{lm_1}|^2 \boldsymbol{G'_{lm_1}}(a,n)|h_{lm_2}|^2 \boldsymbol{G'_{lm_2}}(a,n)\right]\right) \\
&= \frac{\beta_l^2}{M^2}\left(2\sum_{m=1}^{M} E\left[\boldsymbol{G'^2_{lm}}(a,n)\right] + \right. \\
&\qquad \left. \sum_{m_1=1}^{M}\sum_{\substack{m_2=1 \\ m_2\neq m_1}}^{M} E\left[\boldsymbol{G'_{lm_1}}(a,n)\right] E\left[\boldsymbol{G'_{lm_2}}(a,n)\right]\right) \\
&= \frac{\beta_l^2}{M^2}\left(2M\xi''_{a,n} + M(M-1)(\xi'_{a,n})^2\right)
\end{aligned} \tag{90}
$$

where $\boldsymbol{G'}(a,n)$ is defined as follows:

$$
\boldsymbol{G'_{lm}}(a,n) = \sum_{i=1}^{N} \boldsymbol{Z}(a,i) g(e + T + (i-n)T_s - \tau_{lm}) \tag{91}
$$

Afer taking expectations, indices of receive antennas and users are discarded. We denote $E\left[\boldsymbol{G'}^2(a,n)\right]$ as $\xi''_{a,n}$ which is only related to pulse shape, delay distribution and sampling origin and can be calculated numerically. On the other hand, $E\left[\boldsymbol{G'}(a,n)\right]$ which is denoted as $\xi'_{a,n}$ can be calculated analytically as follows:

$$
\begin{aligned}
\xi'_{a,n} &= E\left[\sum_{i=1}^{N} \boldsymbol{Z}(a,i) g(e + T + (i-n)T_s - \tau)\right] \\
&= \sum_{i=1}^{N} \boldsymbol{Z}(a,i) E\left[g(e + T + (i-n)T_s - \tau)\right] \\
&= \sum_{i=1}^{N} \boldsymbol{Z}(a,i) E[g_{i-n}] \\
&= \delta(a-n)
\end{aligned} \tag{92}
$$

Therefore, we will have:

$$
E\left[|\boldsymbol{T}^{\boldsymbol{mrc}}_{\boldsymbol{ll,p}}(a,n)|^2\right] = \frac{\beta_l^2}{M^2}\left(2M\xi''_{a,n} + M(M-1)\delta(a-n)\right) \tag{93}
$$

When $k \neq l$, it can be similarly shown that:

$$E\left[|\boldsymbol{T}^{\boldsymbol{mrc}}_{\boldsymbol{lk,p}}(a,n)|^2\right] = \frac{\beta_l\beta_k}{M^2}(M\xi''_{a,n}) \tag{94}$$

■

Covariance of the noise vector is also calculated by:

$$\begin{aligned} COV[\boldsymbol{n}^{\boldsymbol{mrc-zf}}_{\boldsymbol{l,p}}(a)] &= E\left[\boldsymbol{n}^{\boldsymbol{mrc-zf}}_{\boldsymbol{l,p}}\boldsymbol{n}^{\boldsymbol{mrc-zf}^H}_{\boldsymbol{l,p}}\right] \\ &= E\left[\boldsymbol{Z}\boldsymbol{n}^{\boldsymbol{mrc}}_{\boldsymbol{l,p}}\boldsymbol{n}^{\boldsymbol{mrc}H}_{\boldsymbol{l,p}}\boldsymbol{Z}^H\right] \\ &= \frac{\beta_l}{M}\boldsymbol{Z}\boldsymbol{Z}^H \end{aligned} \tag{95}$$

We denote $\boldsymbol{Z}\boldsymbol{Z}^H(a,a)$ as ϵ_a which is only related to the pulse shape, distribution of delay and origin of sampling. Therefore, by inserting the expectation values and the variance of noise samples, an approximation of the lower-bound on the achievable rate can be calculated as follows:

$$\tilde{R}^{mrc-zf}_{l,p} \approx \log_2\left(1 + \frac{\rho_d\beta_l(2\xi''_{a,a} + (M-1))}{\rho_d(\sum_{n=1}^{N}\xi''_{a,n})\sum_{k=1}^{K}\beta_k + 2\rho_d\beta_l\sum_{\substack{n=1\\n\neq a}}^{N}\xi''_{a,n} + \epsilon_a}\right) \tag{96}$$

Note that due to the structure of system, the achievable rate for different subchannels except the I-boundary ones is same.

APPENDIX D

In the MRC-ZF receiver with imperfect CSI, $\boldsymbol{T}^{\boldsymbol{mrc-zf}}_{\boldsymbol{lk,ip}} = \frac{1}{M}\sum_{m=1}^{M}\sum_{j=1}^{K}\lambda^s_{ljm}\sqrt{\beta_j\beta_k}h^*_{jm}h_{km}\boldsymbol{W_{ll}}\hat{\boldsymbol{G}}_{\boldsymbol{km}}$ where $\boldsymbol{W_{ll}}$ and $\hat{\boldsymbol{G}}_{\boldsymbol{km}} = [(\boldsymbol{G^1_{km}})^T,\ldots,(\boldsymbol{G^K_{km}})^T]^T$ are defined in Section IV-B. The noise vector $\boldsymbol{n}^{\boldsymbol{mrc-zf}}_{\boldsymbol{l,ip}}$ is also equal to $\boldsymbol{W_{ll}}\boldsymbol{n}^{\boldsymbol{os-mrc}}_{\boldsymbol{l,ip}}$.

Lemma 6: The expected value of $|\boldsymbol{T}^{\boldsymbol{mrc-zf}}_{\boldsymbol{lk,ip}}(a,n)|^2$ can be calculated as follows:

$$E\left\{|\boldsymbol{T}^{\boldsymbol{mrc-zf}}_{\boldsymbol{lk,ip}}(a,n)|^2\right\} =$$

$$\frac{1}{M^2}\left\{\beta_k^2\left(2M\hat{\gamma}''_{lkk}(a,n) + M(M-1)(\delta(l-k)\boldsymbol{I_N}(a,n)) + \sum_{\substack{j=1\\j\neq k}}^{K}\beta_j\beta_k(M\hat{\gamma}''_{ljk}(a,n))\right)\right\} \tag{97}$$

Proof: Following the same steps as Lemma 4, replacing $\boldsymbol{G_{km}}$ with $\hat{\boldsymbol{G}}_{\boldsymbol{lkm}} = \boldsymbol{W_{ll}}\hat{\boldsymbol{G}}_{\boldsymbol{km}}$ results in:

$$E\left[|\boldsymbol{T}^{\boldsymbol{mrc-zf}}_{\boldsymbol{lk,ip}}(a,n)|^2\right] =$$

$$\frac{1}{M^2}\left\{\beta_k^2\left(2M\hat{\gamma}''_{lkk}(a,n) + M(M-1)(\hat{\gamma}'_{lkk}(a,n))^2\right) + \sum_{\substack{j=1\\j\neq k}}^{K}\beta_j\beta_k(M\hat{\gamma}''_{ljk}(a,n))\right\} \tag{98}$$

where $\hat{\gamma}''_{ljk}(a,n) = E[\hat{\gamma}^2_{ljkm}(a,n)]$ and $\hat{\gamma}'_{lkk}(a,n) = E[\hat{\gamma}_{lkkm}(a,n)]$ and the expectation is over the delay distributions ($\hat{\gamma}_{ljkm}(a,n) = \lambda^s_{ljm}\hat{\boldsymbol{G}}_{\boldsymbol{lkm}}(a,n)$).

We can calculate $\hat{\gamma}'_{lkk}(a,n)$ analytically as:

$$\begin{aligned}\hat{\gamma}'_{lkk}(a,n) &= \left[\boldsymbol{W_{ll}} E[\lambda^s_{lkm}\hat{\boldsymbol{G}}_{\boldsymbol{km}}]\right](a,n) \\ &= \left[\boldsymbol{W_{ll}}\boldsymbol{\Gamma_{lk}}\right](a,n)\end{aligned} \tag{99}$$

where $\boldsymbol{\Gamma_{lk}} = [(\boldsymbol{\Gamma^1_{lk}})^T, \ldots, (\boldsymbol{\Gamma^K_{lk}})^T]^T$. Because $\boldsymbol{W_l}$ is the inverse of $\boldsymbol{\Gamma_l}$, we can conclude that:

$$\hat{\gamma}'_{lkk}(a,n) = \delta(l-k)\boldsymbol{I_N}(a,n) \tag{100}$$

Therefore, Eq. (98) can be further simplified to:

$$\begin{aligned}&E\left\{|\boldsymbol{T}^{\boldsymbol{mrc-zf}}_{\boldsymbol{lk,ip}}(a,n)|^2\right\} = \\ &\frac{1}{M^2}\left\{\beta_k^2\left(2M\hat{\gamma}''_{lkk}(a,n) + M(M-1)(\delta(l-k)\boldsymbol{I_N}(a,n)\right) + \sum_{\substack{j=1\\ j\neq k}}^{K}\beta_j\beta_k(M\hat{\gamma}''_{ljk}(a,n))\right\}\end{aligned} \tag{101}$$

■

The effective noise vector is equal to:

$$\boldsymbol{n}^{\boldsymbol{mrc-zf}}_{\boldsymbol{l,ip}} = \frac{\sqrt{\rho_d}}{M}\sum_{m=1}^{M}\tilde{n}^s_{lm}\sum_{k=1}^{K}\sqrt{\beta_k}h_{km}\hat{\boldsymbol{G}}_{\boldsymbol{lkm}}\boldsymbol{b_k} + \frac{1}{M}\sum_{m=1}^{M}\left(\sum_{j=1}^{K}\lambda^s_{ljm}\sqrt{\beta_j}h^*_{jm} + \tilde{n}^s_{lm}\right)\boldsymbol{W_{ll}}\boldsymbol{n^{os}_m} \tag{102}$$

where $\hat{n}_{lm}$ is the estimation noise which is Gaussian and its variance is $\frac{1}{\rho_p}$. After some calculations, it can be shown that the variance of the ath element of the noise vector is equal to:

$$VAR[\boldsymbol{n}^{\boldsymbol{mrc-zf}}_{\boldsymbol{l,ip}}(a)] = \frac{\rho_d}{M\rho_p}\sum_{k=1}^{K}\beta_k\boldsymbol{U_l}(a,a) + \frac{1}{M}\left(\sum_{j=1}^{K}\beta_j\lambda''_{lj} + \frac{1}{\rho_p}\right)\boldsymbol{V_l}(a,a) \tag{103}$$

where $\boldsymbol{U_l} = \boldsymbol{W_{ll}}E[\hat{\boldsymbol{G}}_{\boldsymbol{km}}\hat{\boldsymbol{G}}^H_{\boldsymbol{km}}]\boldsymbol{W}^H_{\boldsymbol{ll}}$ and $\boldsymbol{V_l} = \boldsymbol{W_{ll}}\boldsymbol{\Sigma_n}\boldsymbol{W}^H_{\boldsymbol{ll}}$. Finally, by inserting the expected values of the effective channel matrices and also the variance of noise samples into Eq. (75), we derive the following result:

$$\tilde{R}^{mrc-zf}_{l,ip} \approx \log_2\left(1 + \frac{desired\ signal}{IUI + ISI + noise}\right) \tag{104}$$

where the desired signal, ISI, IUI and noise components are defined, respectively as:

$$desired\ signal = \rho_d \beta_l^2 (2\hat{\gamma}''_{lll}(a,a) + (M-1)) + \rho_d \beta_l \sum_{\substack{j=1 \\ j\neq l}}^{K} \beta_j \hat{\gamma}''_{ljl}(a,a)$$

$$ISI = \rho_d \beta_l^2 \sum_{\substack{i=1 \\ i\neq a}}^{N} 2\hat{\gamma}''_{lll}(a,i) + \rho_d \beta_l \sum_{\substack{j=1 \\ j\neq l}}^{K} \beta_j \sum_{\substack{i=1 \\ i\neq a}}^{N} \hat{\gamma}''_{ljl}(a,i)$$

$$IUI = \rho_d \sum_{\substack{k=1 \\ k\neq l}}^{K} \beta_k^2 \sum_{i=1}^{N} 2\hat{\gamma}''_{lkk}(a,i) + \rho_d \sum_{\substack{k=1 \\ k\neq l}}^{K} \sum_{\substack{j=1 \\ j\neq k}}^{K} \beta_k \beta_j \sum_{i=1}^{N} \hat{\gamma}''_{ljk}(a,i)$$

$$noise = \frac{\rho_d}{\rho_p} \sum_{k=1}^{K} \beta_k \boldsymbol{U_l}(a,a) + \left(\sum_{k=1}^{K} \beta_k \lambda''_{lk} + \frac{1}{\rho_p} \right) \boldsymbol{V_l}(a,a)$$

Note that due to the structure of the system, the achievable rate for different subchannels except the I-boundary ones is the same, thus the index of a can be discarded.

REFERENCES

[1] H. Bölcskei, *Space-time wireless systems: from array processing to MIMO communications*. Cambridge University Press, 2006.

[2] T. M. Duman and A. Ghrayeb, *Coding for MIMO communication systems*. John Wiley & Sons, 2008.

[3] H. Jafarkhani, *Space-time coding: theory and practice*. Cambridge university press, 2005.

[4] G. J. Foschini, "Layered space-time architecture for wireless communication in a fading environment when using multi-element antennas," *Bell Labs Technical Journal*, vol. 1, no. 2, pp. 41–59, Autumn 1996.

[5] V. Tarokh, H. Jafarkhani, and A. R. Calderbank, "Space-time block codes from orthogonal designs," *IEEE Transactions on Information Theory*, vol. 45, no. 5, pp. 1456–1467, Jul 1999.

[6] S. Verdu, *Multiuser detection*. Cambridge University Press, 1998.

[7] J. J. van de Beek, P. O. Borjesson, M. L. Boucheret, D. Landstrom, J. M. Arenas, P. Odling, C. Ostberg, M. Wahlqvist, and S. K. Wilson, "A time and frequency synchronization scheme for multiuser ofdm," *IEEE Journal on Selected Areas in Communications*, vol. 17, no. 11, pp. 1900–1914, Nov 1999.

[8] E. Zhou, X. Zhang, H. Zhao, and W. Wang, "Synchronization algorithms for mimo ofdm systems," in *IEEE Wireless Communications and Networking Conference, 2005*, vol. 1, March 2005, pp. 18–22 Vol. 1.

[9] J. J. van de Beek, M. Sandell, and P. O. Borjesson, "Ml estimation of time and frequency offset in ofdm systems," *IEEE Transactions on Signal Processing*, vol. 45, no. 7, pp. 1800–1805, Jul 1997.

[10] A. Das and B. D. Rao, "MIMO Systems with Intentional Timing Offset," *EURASIP Journal on Advances in Signal Processing*, vol. 2011, no. 1, pp. 1–14, 2011.

[11] L. Lu and S. C. Liew, "Asynchronous physical-layer network coding," *IEEE Transactions on Wireless Communications*, vol. 11, no. 2, pp. 819–831, February 2012.

[12] S. Poorkasmaei and H. Jafarkhani, "Asynchronous orthogonal differential decoding for multiple access channels," *IEEE Transactions on Wireless Communications*, vol. 14, no. 1, pp. 481–493, Jan 2015.

[13] M. R. Avendi and H. Jafarkhani, "Differential distributed space-time coding with imperfect synchronization in frequency-selective channels," *IEEE Transactions on Wireless Communications*, vol. 14, no. 4, pp. 1811–1822, April 2015.

[14] M. Ganji and H. Jafarkhani, "Interference mitigation using asynchronous transmission and sampling diversity," in *2016 IEEE Global Communications Conference (GLOBECOM)*, Dec 2016, pp. 1–6.

[15] T. L. Marzetta, "Noncooperative cellular wireless with unlimited numbers of base station antennas," *IEEE Transactions on Wireless Communications*, vol. 9, no. 11, pp. 3590–3600, November 2010.

[16] E. G. Larsson, O. Edfors, F. Tufvesson, and T. L. Marzetta, "Massive mimo for next generation wireless systems," *IEEE Communications Magazine*, vol. 52, no. 2, pp. 186–195, February 2014.

[17] H. Q. Ngo, E. G. Larsson, and T. L. Marzetta, "Energy and spectral efficiency of very large multiuser mimo systems," *IEEE Transactions on Communications*, vol. 61, no. 4, pp. 1436–1449, April 2013.

[18] L. Lu, G. Y. Li, A. L. Swindlehurst, A. Ashikhmin, and R. Zhang, "An overview of massive mimo: Benefits and challenges," *IEEE Journal of Selected Topics in Signal Processing*, vol. 8, no. 5, pp. 742–758, Oct 2014.

[19] F. Rusek, D. Persson, B. K. Lau, E. G. Larsson, T. L. Marzetta, O. Edfors, and F. Tufvesson, "Scaling up mimo: Opportunities and challenges with very large arrays," *IEEE Signal Processing Magazine*, vol. 30, no. 1, pp. 40–60, Jan 2013.

[20] R. Rogalin, O. Y. Bursalioglu, H. Papadopoulos, G. Caire, A. F. Molisch, A. Michaloliakos, V. Balan, and K. Psounis, "Scalable synchronization and reciprocity calibration for distributed multiuser mimo," *IEEE Transactions on Wireless Communications*, vol. 13, no. 4, pp. 1815–1831, April 2014.

[21] A. Pitarokoilis, S. K. Mohammed, and E. G. Larsson, "Effect of oscillator phase noise on uplink performance of large mu-mimo systems," in *2012 50th Annual Allerton Conference on Communication, Control, and Computing (Allerton)*, Oct 2012, pp. 1190–1197.

[22] R. Krishnan, M. R. Khanzadi, N. Krishnan, Y. Wu, A. G. i Amat, T. Eriksson, and R. Schober, "Linear massive mimo precoders in the presence of phase noise-a large-scale analysis," *IEEE Transactions on Vehicular Technology*, vol. 65, no. 5, pp. 3057–3071, May 2016.

[23] A. Pitarokoilis, S. K. Mohammed, and E. G. Larsson, "On the optimality of single-carrier transmission in large-scale antenna systems," *IEEE Wireless Communications Letters*, vol. 1, no. 4, pp. 276–279, August 2012.

[24] Q. Zhang, S. Jin, K. K. Wong, H. Zhu, and M. Matthaiou, "Power scaling of uplink massive mimo systems with arbitrary-rank channel means," *IEEE Journal of Selected Topics in Signal Processing*, vol. 8, no. 5, pp. 966–981, Oct 2014.

[25] B. Hassibi and B. M. Hochwald, "How much training is needed in multiple-antenna wireless links?" *IEEE Transactions on Information Theory*, vol. 49, no. 4, pp. 951–963, April 2003.